Increased Flux through the Hexosamine Biosynthetic Pathway leads to the induction of Acetyl-CoA Caboxylase Gene Expression in the Heart

By Jamie Imbriolo

Thesis presented in partial fulfilment of the requirements for the degree of

Masters of Physiological Sciences at the University of Stellenbosch.

Supervisor: Prof. M. Faadiel Essop

January 2008

Declaration

I, the undersigned, hereby declare that the work contained in this thesis is my own original work and has not previously in its entirety or in part been submitted at any university for a degree.

_____

Signature

_____

Date

Abstract

Gene expression of the cardiac isoform of acetyl-CoA carboxylase (ACCβ) is induced in a glucose-dependent manner. ACCβ produces malonyl-CoA, a potent inhibitor of mitochondrial fatty acid uptake. Previous studies show that increased flux through the hexosamine biosynthetic pathway (HBP) under hyperglycaemic conditions may contribute to the development of insulin resistance. In light of this, we hypothesised that increased HBP flux induces cardiac ACCβ gene expression thereby contributing to the onset of insulin resistance.

We tested our hypothesis by transiently transfecting cardiac-derived rat H9c2 myoblasts with a 1,317 bp human ACCβ promoter-luciferase construct (pPIIβ-1317) and an expression construct encoding the rate-limiting step of the HBP i.e. glutamine: fructose 6-phosphate amidotransferase (GFAT). Overexpression of GFAT increased ACCβ gene promoter activity by 75 ± 23% versus controls (n=6, $p<0.001$). When co-transfection experiments were repeated in the presence of varying concentrations of L-glutamine (0 mM, 4 mM, 8 mM), a substrate for the HBP, ACCβ promoter activity was dose-dependently increased. To further corroborate these findings, we employed two inhibitors of GFAT, i.e. 40 µM azaserine and 40 µM 6-diazo-5-oxo-L-norleucine were administered to transfected cells for a period of 24 hours. Here both azaserine and 6-diazo-5-oxonorleucine attenuated ACCβ gene promoter activity.

In agreement, co-transfections with two dominant negative GFAT constructs also diminished ACCβ gene promoter activity. We next inhibited two enzymes of the HBP acting downstream of GFAT, i.e. O-GlcNAc transferase and O-GlcNAcase using alloxan (0.1 mM, 1 mM and 2 mM) and streptozotocin (5 mM and 10 mM),

respectively, for a period of 24 hours. Addition of alloxan attenuated ACCβ gene promoter activity by 35.6 ± 1.9% (n=16, $p<0.001$) and streptozotocin increased activity by 32 ± 12% (n=12, $p<0.001$). We also investigated USF1 and USF2 as transcriptional regulatory candidates for HBP-induced ACCβ promoter regulation. Our data implicates USF2 as an important transcriptional regulator of HBP-induced ACCβ promoter regulation.

In summary, this study demonstrates that increased flux through the hexosamine biosynthetic pathway induces ACCβ gene promoter activity. We further propose that such an induction would reduce cardiac fatty acid oxidation, thereby leading to intracellular lipid accumulation due to a mismatch between sarcolemmal FA uptake and mitochondrial FA oxidation in the insulin resistant setting (i.e. hyperlipidaemia).

Opsomming

Geen uitdrukking van die kardiale isoform asetiel-KoA karboksilase (ACCβ) word in ‘n glukose afhanklike wyse geïnduseer. ACCβ produseer maloniel-KoA, ‘n kragtige inhibeerder van mitochondriale vetsuuropname. Vorige studies toon aan dat verhoogde fluks deur die heksosamien biosintestiese weg (HBW) onder hiperglukemiese toestande bydra tot die ontwikkeling van insulienweerstand. In die lig hiervan, word daar gehipotetiseer dat verhoogde HBP fluks kardiale ACCβ geenuitdrukking induseer en so bydra tot die ontstaan van insulienweerstand.

Ons hipotese is getoets deur die kardiale afkomstige rot H9c2 mioblaste met ‘n 1.317 bp mens ACCβ-lusiferase promotor konstruk (pPII-1317) te transfekteer en ‘n uitdrukking te konstrueer wat die tempo bepalende stap van HBP i.e. glutamien: fruktose-6-fosfaat amidotransferase (GFAT) kodeer. Ooruitdrukking van GFAT verhoog ACCβ geenpromotor aktiviteit deur 75 ± 23% teenoor kontrole (n=6, $p<0.001$). Die herhaling van ko-transfeksie eksperimente is herhaal in die teenwoordigheid van variëerbare L-glutamienkonsentrasies (0 mM, 4 mM, 8 mM), ’n substraat vir die HBP, ACCβ promotor aktiwiteit is dosisafhanglik verhoog. Om die bevindinge verder te staaf, is twee inhibeerders van GFAT, i.e. 40 µM azaserien en 40 µM 6-diazo-5-oxo-L-norleusien aan transfeksie selle toegedien vir ’n tydperk van 24 uur. Beide azaserien en 6-diazo-5-oxo-L-norleusien verlaag ACCβ geenpromotor aktiwiteit.

In ooreenstemming met die bogenoemde het ko-transfeksies met twee dominante negatiewe GFAT konstrukte ook ACCβ geenpromoter aktiwiteit verminder. Die volgende stap is om twee ensieme van die HBP wat stroomaf van GFAT aktief is, vir

‘n periode van 24 uur te inhibeer i.e. O-GlcNAc transferase en O-GlcNAcase deur alloxan (0.1 mM, 1 mM en 2 mM) and streptozotosien (5 mM en 10 mM) onderskeidelik vir ‘n 24 uur periode te gebruik. Toevoeging van alloxan het die ACCβ geenpromotor aktiwiteit by 35.6 ± 1.9% (n=16, $p<0.001$) verlaag en streptozotosien aktiwiteit verhoog by 32 ± 12% (n=12, $p<0.001$). Ons het ook die USF1 en USF2 as transkripsie regulerings kandidate vir HBP-geïnduseerde ACCβ promotor regulering ondersoek. Ons data impliseer dat USF2 as ‘n belangrike transkripsie reguleerder van HBP-geïndiseerde ACCβ promotor regulering is.

Samevattend het hierdie studie demonstreer dat verhoogde fluks deur die hexosamien biosintetiese weg ACCβ geenpromotor aktiwiteit induseer. Ons stel verder voor dat hierdie induksie die kardiale vetsuuroksidasie verlaag wat daartoe lei dat intrasellulêre lipied akkumulasie as gevolg van onparing tussen sarkolemma vetsuuropname en mitochondriale vetsuuroksidasie in ’n insulien weerstandige situasie (i.e. hiperlipidaemia).

I dedicate this thesis to my twin sister, Lucille and to my two nephews, Jesse and Michael.

Acknowledgements

I would like to thank my supervisor, Prof. Faadiel Essop, for his unwavering support and patience. Thanks for the opportunity to learn something new. You gave me the right balance of leadership, allowing me to explore the answers on my own while keeping me focussed on the task at hand.

I'd like to thank my mother for encouraging me to never give up. If I didn't have you I don't know what I would do. Thank you for having the patience to put up with my various mood swings.

I would like to thank the academic staff at the Department of Physiological Sciences for their great leadership. Their decisions have resulted in a high class research environment that is both educationally stimulating and fun.

Dr. James Meiring for proof reading this thesis.

Dr. Theo Nell for help in translating my abstract from English to Afrikaans.

I would like to thank Dr. Rob Smith for making it possible to live in Bergvliet and work in Stellenbosch.

Wing-Win Anna Chan, "Tsunami", for providing the db/db mouse samples. Also for the interesting Chinese sweeties and tea, and yes, you are still my favourite Chinese girl.

Tasneem Adam, for your help in being a source of technical assistance and a true friend. Without you I doubt this project would have gotten anywhere.

Lydia Lycerda, for teaching me the “ins and outs” of cell culture. There is no better person from which to learn this technique.

To my new friends at the Physiology Department of Stellenbosch University: Mark (“The Pretzel man”) Thomas, the best way to lighten the mood. Gustavus III van Niekerk, for asking the question: “Yes, I know it works… but how can I make it better?” Celeste Fouche and Maritza Jacoba Kruger, a rare combination of spicy chilli and sugar. I won’t say which is which.

I would like to thank Shaun Knight and Andrezj Michalski. It’s rare to have the same friends for more than half your lifespan. Thanks for your support.

I would like to thank the coffee bean. We did not know each other so well until this thesis began.

Lastly, I would like to thank God for the chance of a life time to make friends, to make new friends and for challenging me with the various “trials and tribulations” of the past two years. If we live life unchallenged, we fail to grow and I have grown tremendously because of it.

Table of Contents

Abbreviations

ACBP	Acyl-CoA binding protein
ACC	Acetyl-CoA carboxylase
acetyl-CoA	Acetyl-Coenzyme A
Acyl-CoA	Acyl-Coenzyme A
AMP	adenosine monophosphate
AMPK	AMP-activated protein kinase
ATP	Adenosine triphosphate
BSA	Bovine serum albumin
CACT	Carnitine/acylcarnitine transferase
ChREBP	Carbohydrate response element-binding protein
CPT	Carnitine palmitoyl transferase
CTD	Carboxyl-terminal domain
dGFAT	Dominant negative GFAT
dH_2O	Distilled water
DMEM	Dulbecco's modified Eagle's medium
DNA	Deoxyribonucleic acid
DNL	*De novo* lipogenesis
DON	6-Diazo-5-oxo-L-norleucine
ECL	Enhanced chemiluminescence
EDTA	Ethylene diamine tetraacetic acid
eIF	Eukaryotic factor
ER	Estrogen receptor
F-6-P	Fructose-6-phosphate

FABP	Fatty acid binding protein
$FADH_2$	Flavin adenine dinucleotide
FAS	Fatty acid synthase
FAT	Fatty acid transporter
FATP	Fatty acid transport protein
FCS	Fetal calf serum
FFA	Free fatty acids
GFAT	Glutamine: fructose 6-phosphate amidotransferase
Glc-6-P	Glucose-6-phosphate
GlcN-6-P	Glucosamine-6-phosphate
GlcNAc	*N*-acetylglucosamine
GLUT	Glucose transporter
GP	Glycogen phosphorylase
GS	Glycogen synthase
H_2O	Water
HBP	Hexosamine biosynthetic pathway
HCl	Hydrogen chloride
H-FABP	Heart-type fatty acid binding protein
HK	Hexokinase
HRP	Horse-radish peroxidase
IRS-1	Insulin receptor 1
kDa	kilodaltons
LCFAs	Long-chain fatty acids
LAR	Luciferase assay reagent
malonyl-CoA	Malonyl-Coenzyme A
MCD	Malonyl-Coenzyme A decarboxylase

mg	Milligrams
ml	Millilitre
mM	Millimolar
mRNA	Messenger ribonucleic acid
n	Numbers
NADH	Nicotinamide adenine dinucleotide
nm	Nanometer
O-GlcNAc	O-linked β-*N*-acetylglucosamine
O-GlcNAcase	β-*N*-acetylglucosaminidase
OGT	O-linked β-*N*-acetylglucosaminyl transferase
PDH	Pyruvate dehydrogenase
PFK	Phosphofructokinase
PI-3 kinase	Phosphoinositide 3-kinase
PMSF	Phenylmethylsulfonyl flouoride
PPARs	Peroxisome proliferator-activated receptors
PPP	Pentose phosphate pathway
Pro	Proline
PUGNAc	O-(2-acetamido-2-deoxy-D-glucopyranosylidene) amino-*N*-phenylcarbamate
PVDF	Polyvinylidene difluoride
RIPA	Radio immuno precipitation assay
RNA	Ribonucleic acid
RNA Pol	Ribonucleic acid polymerase
rpm	Revolutions per minute
RT	Room temperature
RT-PCR	Real-time polymerase chain reaction

SBT	Strontium bismuth tantalate
SDS	Sodium dodecyl sulphate
Ser	Serine
STZ	Streptozotocin
TBS	Tris-buffered saline
Thr	Threonine
Tyr	Tyrosine
UDP	Uridine diphospho
UDP-GlcNAc	Uridine diphospho-*N*-acetylglucosamine
µl	Microlitre
USF	Upstream stimulatory factor
VLDLs	Very-low density lipoproteins

List of Tables

List of Figures

Chapter 1

Introduction

1.1 Epidemiology

Obesity is defined as an excess of body fat which accumulates in adipose tissue, associated with increased fat cell size and number (68). Obesity has become more prevalent world wide, resulting in an increase in related diseases such as type-2 diabetes. Although obesity is especially common in industrialised countries, its prevalence is also dramatically increasing in developing countries such as South Africa (4). The movement of populations from a rural type to a more “western-based” lifestyle with its increased availability of high-calorie foods is a key factor that has lead to a higher incidence of obesity. It is predicted that ~300 million people worldwide will be diagnosed with type-2 diabetes by 2025 (122, 126).

Most patients who are obese develop insulin resistance which is characterised as an impairment of insulin to mediate glucose uptake and metabolism by muscle and adipose tissue. Cardiovascular disease is the primary cause of mortality in obese individuals and in patients diagnosed with type-2 diabetes mellitus (60, 68, 112, 127). Although the heart plays a small role in the development of insulin resistance throughout the whole body, cardiovascular complications are the main causes of death in insulin resistant obese and type-2 diabetes patients (23). Diabetes mellitus is a cluster of metabolic perturbations characterized by high blood glucose levels or hyperglycaemia, which result from defects in insulin secretion, or action, or both. Diabetes mellitus, can easily be identified with high glucose levels found in urine and excessive muscle loss (121).

South Africa has a unique, heterogeneous population originating from a diverse range of ethnic backgrounds. The ~ 46 million individuals that reside in South Africa largely consist of African (79%), Caucasoid (9.6%), mixed ancestry (“coloured”) (8.9%) and Indian backgrounds (2.5%). More recently, migrants from other African countries have also settled in South Africa. This diverse cultural and ethnic diversity makes it difficult to elucidate trends with respect to changes in diet and health behaviours of the entire population. There are also limited studies performed to assess the prevalence of metabolic syndrome (a precursor to obesity and diabetes) in South Africa. However, recent data show that mortality rates from ischaemic heart disease among whites, coloureds and Indians were found to be more than 2x the rate for blacks, while stroke death rates among blacks and coloureds were double compared to whites (Table 1).

There are many sociological implications why the prevalence of cardiovascular diseases has become more common. For example, for the black community, the highest incidences of obesity are observed in black women (4). This may, in part, depend on the cultural background in the black population where obesity is often regarded as a reflection of health and wealth (4).

Table 1: Age-standardised mortality rates per 100, 000 population, South Africa (112).

	Ischaemic heart disease	Stroke	Hypertensive heart disease	Diabetes
Black	70	143	88	56
White	230	72	10	22
Coloured	171	139	37	59
Indian	392	392	29	103
South Africa	123	124	68	54

Other associated lifestyle risk factors may also influence the epidemiology of cardiovascular diseases. Risk factors such as physical inactivity, increased smoking, hypertension and hypercholesterolemia may play an important role in the increase in cardiovascular disease and type-2 diabetes (112, 131). For example, although measures were adopted to reduce smoking (higher retail prices and a smoking ban) a recent South African report found that the prevalence of young smokers (14 years) increased by 30% (112). The survey was performed from 1998 to 2003 among a population of 15,124 school children in South Africa. Furthermore, the prevalence of sedentary behaviour has increased in recent years (112). Together these data highlight the increased burden of diabetes and cardiovascular diseases faced by developing nations such as South Africa.

In light of this our laboratory has begun to investigate the basic mechanisms underlying the development of diabetes and cardiovascular diseases. In particular, we are focusing on the role of altered metabolism in the pathogenesis of type-2 diabetes and heart diseases. For the next part of this Introduction, I will now review some basics aspects of the heart's metabolism and thereafter focus on my particular interest, i.e. the hexosamine biosynthetic pathway.

1.2 Metabolism of the heart

The heart pumps blood for the complete lifespan of an individual. This constant workload demands a high capacity for energy production in the form of adenosine triphosphate (ATP), produced by the mitochondria of the heart. In terms of its fuel substrate preferences, the heart is like an omnivore, utilising fatty acids, glucose, lactate and ketone bodies and is able to switch between either one depending on substrate availability (23). The normal adult mammalian heart prefers fatty acids as a fuel source, i.e. obtaining ~70% of its energy from fatty acid oxidation with the remainder provided by glucose and lactate (23). In the foetal heart carbohydrates are major substrates.

The heart utilises ketone bodies as a fuel source during fasting conditions. Metabolism of ketones generates $NADH_2$ and $FADH_2$ which can be used to generate energy by the electron transport chain (36). It has been shown that ketone bodies are able to suppress cardiac fatty acid oxidation in diabetes (46).

Studies have shown that in conditions of increased exercise, hypoxia, and anoxia excess pyruvate from glycolysis is converted into lactate (37). Brooks et al. (2000) introduced the hypothesis of a ‘’lactate shuttle’’ (9). This hypothesis proposes that lactate formation and its distribution throughout the body can act as a mechanism to coordinate metabolism in different tissues. It is known that during intense exercise lactate flux can exceed glucose flux (9, 37).

1.2.1. Fatty acid metabolism

Fatty acids have four major physiological roles in metabolism. Firstly, it forms building blocks in the formation of phospholipids and glycolipids; secondly its involved in the modification of proteins that are targeted to the cell membrane; thirdly it can serve as hormones and intracellular messengers; and finally fatty acids are utilised as fuel substances (113). Fatty acids are stored as triacylglycerol in adipose tissue until it is needed, i.e. then to be broken down by lipolysis (113).

Long-chain fatty acids (LCFAs) enter the circulation in two forms, either in a complex with albumin or esterified in a lipid core of very-low density lipoproteins (VLDLs) and chylomicrons (23, 109, 118). Free fatty acids (FFA) are released into the bloodstream by adipose tissue and taken up by non-adipose tissue via sarcolemmal transporters. It was first believed that LCFAs were transported across the sarcolemma into cardiomyocytes by passive diffusion, but it is now accepted that most of LCFAs are taken up by membrane transporters (40, 72, 73, 92). Two such fatty acid transporters are fatty acid translocase, a rat homologue of human CD36 (FAT/CD36) and fatty acid binding protein (FABP) (8, 82). There are also two isoforms of the fatty acid transport protein (FATP) family, i.e. FATP1 and FATP6 present in cardiomyocytes (110). Both exhibit acyl-CoA synthetase activity. FATP6 is found exclusively and in higher abundance in the heart. FATP has been found to colocalise with FAT/CD36 and both these LCFA transport proteins act in concert with each other.

Once inside the cardiac myocyte, LCFAs bind to a cytoplasmic heart-type fatty acid binding protein (H-FABP). This protein transports non-esterified LCFAs towards a site where they are converted and activated by acyl-Coenzyme A (acyl-CoA) synthetase to form fatty acyl-CoA. Acyl-CoA binding protein (ACBP) then binds to these acyl-CoAs and can either incorporate acyl-CoA into intracellular lipid pools or shuttle it to the mitochondria to be metabolised.

Fatty acyl-CoA is transported into the mitochondria by the action of three proteins which function as a complex. At the outer membrane is carnitine palmitoyl transferase (CPT1) which catalyses the formation of acylcarnitine (23, 29). Connected to CPT1 is carnitine/acylcarnitine transferase (CACT) which transports acylcarnitine into the mitochondria. The final enzyme (CPT-II) is found on the inner mitochondrial membrane and releases acyl-CoA into the mitochondrial matrix (23). The process of mitochondrial LCFA uptake is regulated by CPT1 which is the rate-limiting enzyme for this process (Figure 1).

After uptake is complete the acyl-CoAs are oxidised by β-oxidation producing acetyl-CoA as a by-product. Acetyl-CoA from β-oxidation enters the citric acid cycle to be degraded along with acetyl-CoA from glucose oxidation (23, 34, 103). The result is the generation of $FADH_2$ and NADH that enter the mitochondrial respiratory chain. In oxidative phosphorylation, ATP synthesis is coupled to the flow of electrons from NADH or $FADH_2$ to oxygen by a proton gradient across the inner mitochondrial membrane.

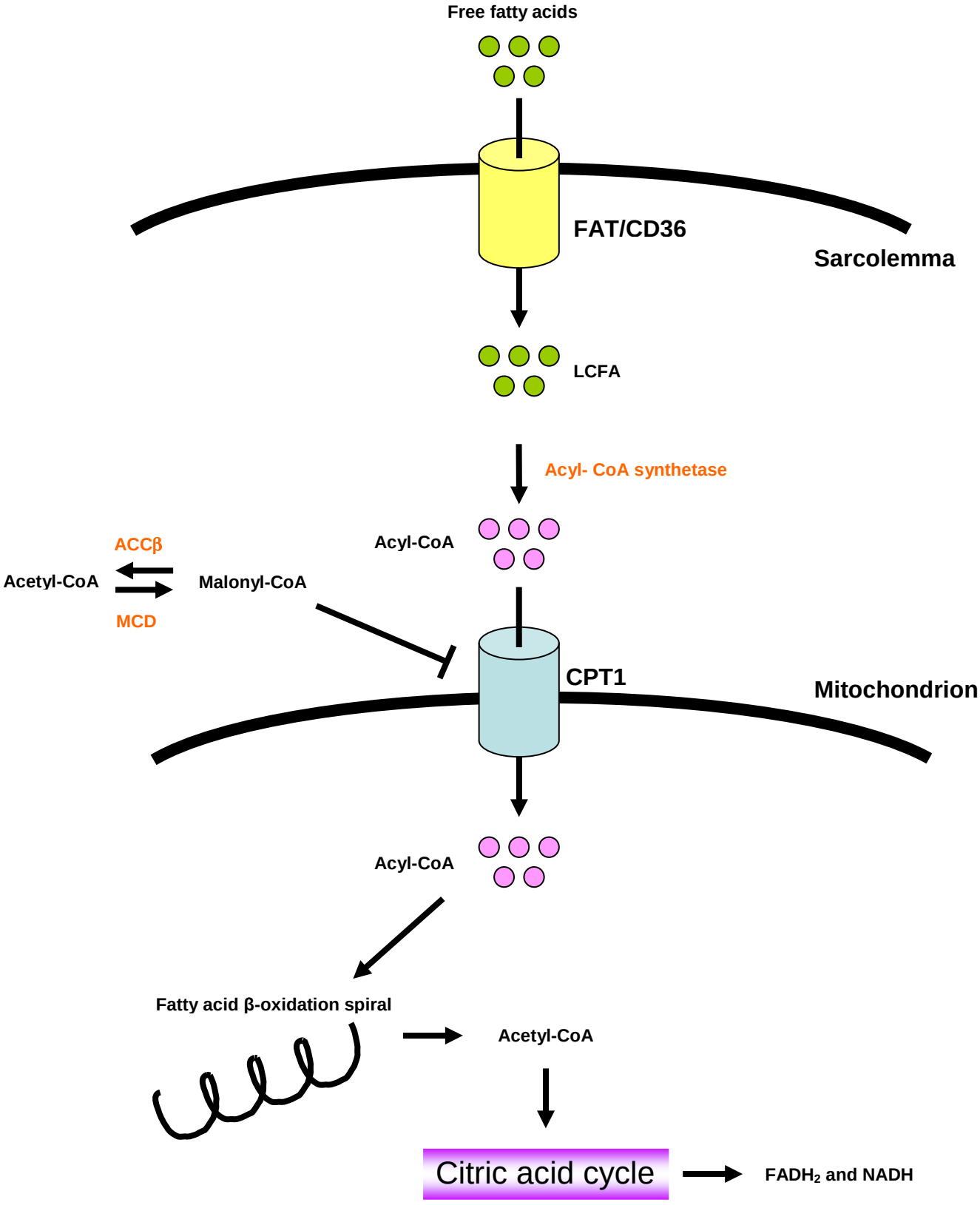

Figure 1: Diagram of fatty acid metabolism.
(CPT1: carnitine palmitoyl transferase, ACCβ: acetyl-coenzyme A carboxylase β, LCFA: long-chain fatty acid).

A proton gradient is created by pumping protons out of the mitochondrial matrix into the inter-mitochondrial membrane space. Thus a proton gradient is formed which creates a membrane potential. The protons then flow back into the mitochondrial matrix through ATP synthase which drives ATP production (113).

Even though LCFAs are utilised for energy production they also play a role in the regulation of genes involved in their own metabolic pathway. LCFAs induce genes that increase fatty acid oxidation by activating a family of ligand-activated nuclear receptors called the peroxisome proliferator-activated receptors (PPARs) (114, 117). There are three isoforms of PPARs, i.e. PPARα, β/δ and γ (114, 117). PPARα and β/δ are the main isoforms expressed in cardiomyocytes and activation of these genes results in an increased expression of regulators of fatty acid oxidation and fatty acid uptake, i.e. FAT/CD36 and CPT1 (35).

Fatty acid oxidation is regulated depending on fatty acid availability, its uptake by mitochondria and by its breakdown. Mitochondrial uptake of long-chain fatty acyl units is controlled by CPT1. A key molecule responsible for the regulation of CPT1 is malonyl-CoA (66, 68, 89, 100, 111, 130). Malonyl-CoA is a potent inhibitor of CPT1 and is produced from acetyl-CoA by an enzyme known as acetyl-CoA carboxylase (ACC) (66, 68, 89, 100, 111, 130). Another enzyme, malonyl-CoA decarboxylase (MCD) degrades malonyl-CoA into acetyl-CoA (28, 111). ACC has two isoforms, ACCα and ACCβ, that have different physiological roles based on their distinct subcellular distributions (44).

ACCα is a cytosolic enzyme (molecular mass of 265 kDa) that supplies malonyl-CoA to fatty acid synthase (FAS) and is committed to *de novo* lipogenesis (DNL) in many tissues via subsequent nutritional and hormonal regulation (3, 39, 44, 61, 97). In contrast, ACCβ (molecular mass of 280 kDa) is anchored to the mitochondrial surface via a unique N-terminal domain that includes 20 hydrophobic amino acids (1, 2, 39, 44). ACCβ is responsible for malonyl-CoA production in the heart. ACCβ overexpression increases malonyl-CoA production resulting in a decrease in fatty acid uptake (28, 66, 89, 100, 111, 130). AMP-activated protein kinase (AMPK) plays and important role in the regulation of CPT1 by phosphorylating and inhibiting ACCβ, resulting in an increase in fatty acid oxidation. Phosphorylation of ACCβ by AMPK is well documented (27, 54). It has been suggested that MCD is also phosphorylated by AMPK (27, 101). Therefore, AMPK plays a distinct and important role in regulating both malonyl-CoA levels and fatty acid oxidation in the heart.

ACCβ is expressed abundantly in heart, skeletal muscle, and liver (1, 61, 87, 133). ACCβ transcripts contain two species of 5'-UTRs, which contain either the sequence of exon 1a or of exon 1b via the alternative usage of two promoters, i.e. promoter 1 and promoter 2 (P1 and P2) (87). Exon 1a and exon 1b are located ~ 15 kilobases apart in human genome but are both connected to exon 2 in mRNA after splicing (87). However, they both use the same ATG start codon for translation, which is found in exon 2 and therefore the two transcripts encode for the same protein (39, 67, 87). A differential regulation of ACCβ gene expression originates from alternative usage of promoters, such as P1 and P2 in different tissues. P1 is the sole promoter

found in the heart and skeletal muscle of rats, although both P1 and P2 are active in human skeletal muscle (87).

In human skeletal muscle and P2 is regulated by myogenic regulatory factors (MRFs) (67, 87). MRFs, including Myf5, MyoD, myogenin, and MRF4, are basic helix-loop-helix transcription factors involved in myogenic differentiation. These factors all recognize the same consensus sequence, i.e. E-box (CANNTG) (87). Myogenin and MRF4 play a major role in the expression of muscle genes in fully differentiated myotubes, while Myf5 and MyoD have been shown to establish the myogenic lineage during embryogenesis (87, 98, 99, 102, 108). It is important to note that myogenic regulatory factor-binding sites found in the human ACCβ P2 are not conserved in rat P2. This would contribute to this difference in P2 usage between human and rat skeletal muscle (87).

The level of ACCβ is higher in the heart than in skeletal muscle. It is currently not known which promoter controls ACCβ expression in the heart. Cardiomyocyte-specific transcription factors, such as Csx/Nkx2.5, GATA4, MEF2, and eHand have been implicated in cardiac development and cardiac gene expression. Unlike in skeletal muscle MRFs have not been shown to be involved in this regulation (58, 63, 84, 87, 88).

The nucleotide sequence of the cDNA of the human liver ACCβ carboxylase has an open reading frame of 7,449 nucleotides that encode 2,483 amino acids. The nucleotide sequences and the predicted amino acid sequences

from the cDNA of ACCβ, has ~60 and 80% in similarity to that of ACCα, respectively. Ser77 and Ser79 have been found to be critical for the phosphorylation and of rat ACCα (Ser78 and Ser80 of human ACCα) (1, 87). These amino acids are conserved in ACCβ and are represented as Ser219 and Ser221, respectively. Another phosphorylation site, Ser1200, in rat ACCα (Ser1201 of human ACCα) has been found to be absent in ACCβ.

Most of the homology between the amino acid sequences of the human ACC isoforms is found downstream of residues Ser78 and Ser81 in human ACCα and their equivalent residues in ACCβ, i.e. Ser219 and Ser221 (1). It has been suggested that the first 218 amino acids at the N terminus of ACCβ represents a unique peptide that could be responsible for the variation between the two carboxylases (1). Despite the similarities between these two isoforms, studies with rat liver ACCα and ACCβ showed that the two isoforms do not cross-react immunochemically (1, 128). It was shown that when the amino acid sequences of the human ACCα and ACCβ are aligned, an extra 142 amino acids can be found in ACCβ (i.e. 426 bp in ACCβ cDNA) (1, 87). It is believed that the extra 142 amino acids are involved in controlling the localisation of ACCβ in the cell, i.e. to the mitochondrion.

1.2.2. Glucose metabolism

The uptake of extracellular glucose by myocytes is mediated by glucose transporters (GLUTs). There are two glucose transporters that can be found in the heart, i.e. GLUT1 and GLUT4 that are located not only in the sarcolemma but also in intracellular storage compartments (6, 23, 48-50, 62, 77, 78, 80, 105). GLUT1 is the foetal isoform and can be found in less abundance than the adult, insulin-stimulated glucose transporter (GLUT4). After glucose has entered the cardiomyocytes it is rapidly phosphorylated by hexokinase into glucose-6-phosphate.

Once converted to glucose-6-phosphate, glucose can be metabolised in six different ways (Figure 2). Firstly, glycogen synthesis can take place and glucose-6-phosphate can be converted by glycogen synthase (GS) into glycogen for storage. This process is reversible and when required glycogen phosphorylase (GP) can convert glycogen back into glucose-6-phosphate (113). Some of the glucose-6-phosphate can enter the pentose phosphate pathway (PPP) where it has been proposed that xylulose-5-phosphate activates a specific isoforms of protein phosphatase 2A which, in turn, dephosphorylates the transcription factor carbohydrate response element-binding protein (ChREBP) (53, 129). In the liver ChREBP translocates from the cytosol to the nucleus where it regulates the expression of glycolytic and lipogenic enzymes (57).

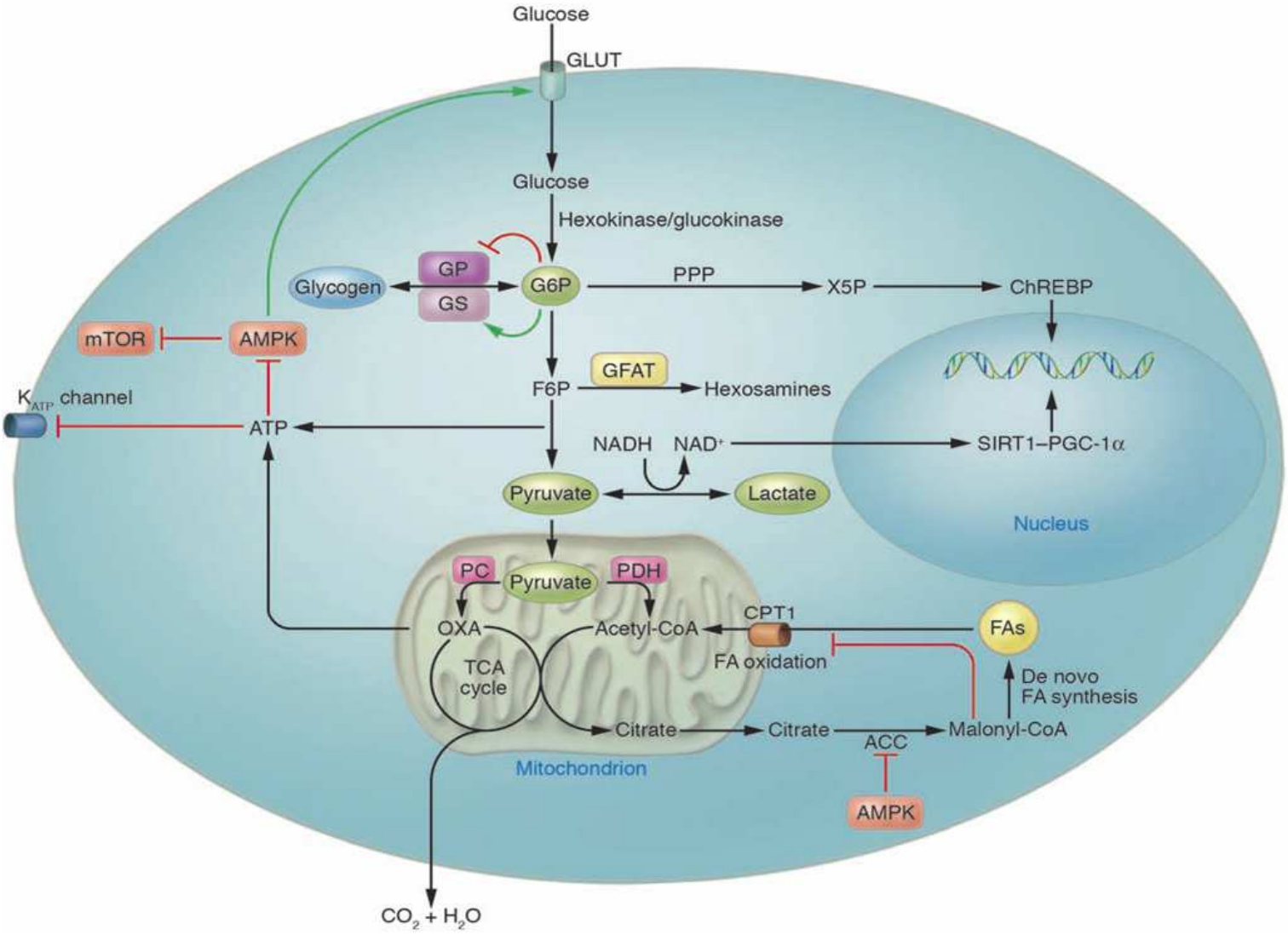

Figure 2: Diagram representing the different pathways of glucose metabolism (reproduced from (53)).

Most of the glucose-6-phosphate enters glycolysis. After the first step of glycolysis, phosphoglucose isomerase converts glucose-6-phosphate into fructose-6-phosphate (Figure 2). At this point most of the fructose-6-phosphate continues down the glycolytic pathway where it is converted to pyruvate after a long series of steps. However, a small percentage of the fructose-6-phosphate is diverted to another pathway responsible for nutrient sensing, i.e. the hexosamine biosynthetic pathway (77, 95) (to be discussed in more detail later).

In the glycolytic pathway, fructose-6-phosphate is converted into fructose-1,6-bisphosphate by phosphofructokinase which is the rate-limiting enzyme of glycolysis (113). The production of pyruvate marks the end of the glycolytic pathway. In the absence of oxygen pyruvate can be reversibly converted to lactate. Under aerobic conditions pyruvate is transported into the mitochondria by pyruvate dehydrogenase (PDH), the rate limiting enzyme of glucose oxidation, where it undergoes oxidative decarboxylation into acetyl-CoA (113). Acetyl-CoA from glucose metabolism, together with acetyl-CoA from fatty acid oxidation, enters the citric acid cycle (Krebs cycle) where it is oxidised to carbon dioxide, NADH and $FADH_2$. The NADH and $FADH_2$ produced are then used in oxidative phosphorylation to produce ATP after donating their electrons to oxygen (113).

Another pathway that utilizes glucose is the polyol pathway. The polyol pathway consists of two steps in which glucose is converted to sorbitol and then converted into fructose (70). During this process NADPH is converted to $NADP^+$ (70). The polyol pathway mainly functions to remove excess glucose from glycolysis and then return it to the glycolytic pathway again (70).

The glyoxylate pathway is found mainly in plants and yeast (69). This pathway converts acetyl-CoA into oxoloacetate by bypassing the steps in the citric acid cycle. It can therefore use fats for the synthesis of carbohydrates (69).

The last pathway that utilises carbohydrates is the biosynthesis of oligosaccharides and glycoproteins which are then expressed on the surface of cell membranes (20).

1.2.3 The Randle cycle

The Randle cycle (named after Philip Randle, its first proposer), which has been used to explain the reciprocal relationship between fatty acid oxidation and glucose oxidation, has long been implicated as a potential mechanism for hyperglycaemia and type-2 diabetes mellitus (106). The Randle cycle states that increased fatty acid oxidation causes a decrease in glucose oxidation. Thus in the setting of excess FFA and glucose supply (insulin resistant state), this is thought to lead to lower glucose uptake and eventually hyperglycaemia (106). Here, acetyl-CoA and NADH derived from fatty acid oxidation can suppress pyruvate oxidation by inhibiting pyruvate dehydrogenase (33, 85). Increased fatty acid oxidation has also shown to result in the inhibition of phosphofructokinase and prevent glycolysis. This would increase glucose flux through other glucose pathways and result in glucose accumulation (85).

1.2.4. Hexosamine biosynthetic pathway

Since the focus of my thesis is on the hexosamine biosynthetic pathway, I will now discuss this in more detail. The hexosamine biosynthetic pathway (HBP) is a relatively small branch glucose utilising pathway. Only ~3% of the total glucose utilised in the cell enters the HBP (77, 95). The pathway is catalysed by the rate-limiting enzyme glutamine: fructose 6-phosphate amidotransferase (GFAT). During this first step, fructose-6-phosphate and glutamine is converted to glucosamine-6-phosphate and glutamate (Figure 3). Thereafter, through a series of steps glucosamine-6-phosphate is converted to glucosamine-1-phosphate. After the addition of uridine, it is converted into uridine diphospho-*N*-acetylglucosamine (UDP-GlcNAc) and CMP-sialic acid. UDP-GlcNAc is the end product of the HBP pathway and also functions as an inhibitor of GFAT (12).

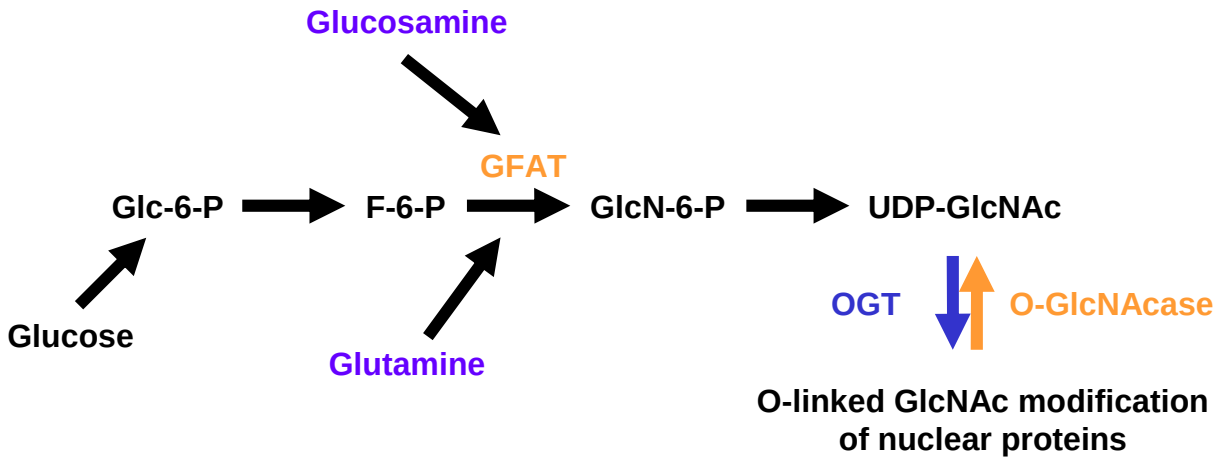

Figure 3: Description of the hexosamine biosynthetic pathway.
(GFAT: glutamine:fructose-6-phosphate amidotransferase, OGT: O-linked β-*N*-acetylglucosaminyl transferase, O-GlcNAcase: β-*N*-acetylglucosaminidase).

UDP-GlcNAc functions as the substrate for O-linked β-*N*-acetylglucosamine transferase (OGT). OGT catalyses the reversible modification of various proteins and transcription factors by cleaving UDP from GlcNAc and transferring GlcNAc in O-linkage to serine/threonine residues on proteins (12, 64, 71). O-GlcNAc modification has two novel mechanisms of action. Firstly, O-GlcNAc is not elongated into a more complex structure (115). Secondly, it has a nucleoplasmic distribution instead of being localised to the cell surface like other glycoproteins (45, 52). O-GlcNAc modification has been implicated in modulating different mechanisms that include (i) regulating protein phosphorylation and function; (ii) altering protein degradation; (iii) altering the localisation of proteins; (iv) modulating protein-protein interactions and (v) mediating transcription (132).

The sites of O-GlcNAc modification are often identical or adjacent to known phosphorylation sites, suggesting that “O-GlcNAcation” plays a role in regulation of a wide range of pathways (12, 125). It has been shown that O-GlcNAc regulation can modify proteins in competition with phosphorylation (21). In some instances O-GlcNAc and phosphorylation can exist on separate and distinct subsets of a protein. For example, c-Myc and RNA polymerase both contain threonine or tyrosine sites that can be phosphorylated or glycosylated, but although, there has been no proof that the two modifications can exist on one protein, there is a possibility that this dual-protein modification can occur. In particular, RNA polymerase II exists in two distinct forms, i.e. RNA Pol IIA and RNA POL IIO (21, 132). RNA polymerase II contains a highly conserved carboxyl-terminal domain (CTD) consisting of 52 tandem repeats of the consensus sequence Tyr-Ser-Pro-Thr-Ser-Pro-Ser (21, 24, 26, 132). The CTD of the IIO isoforms is found to be phosphorylated on

the serine and threonine residues. In contrast, the IIA isoform is non-phosphorylated and exhibits extensive O-GlcNAc modification. The existence of both O-GlcNAc and phosphorylation site implies a precise regulation of protein activity (21).

The modifications of proteins by OGT with O-GlcNAc are also closely regulated. Another enzyme responsible for the regulation of O-GlcNAcation is β-*N*-acetylglucosaminidase (*O*-GlcNAcase). Although OGT is responsible for binding O-GlcNAc to serine/threonine residues of proteins, O-GlcNAcase functions to remove O-GlcNAc. O-GlcNAc modification is thus regulated in the same manner as phosphorylation (Figure 3).

O-GlcNAc modification targets numerous proteins, including transcription factors (21, 132). For example, Sp1, an important transcription factor in the regulation of several target genes, has been shown to have multiple O-GlcNAc residues (12, 21, 132). O-GlcNAc has been shown to alter protein degradation by two different mechanisms, i.e. (i) by altering the targeting of proteins to the proteasome or (ii) by altering the activity of the proteasome. O-GlcNAc modifies eukaryotic factor (eIF) 2α-p67, Sp1 and estrogen receptor (ER)-β prolonging the half-life of these proteins (132). Insulin has been reported to increase O-glycosylation and nuclear content of Sp1 (74).

Incubation with high glucose or increasing flux through HBP by overexpressing GFAT increased the expression of upstream stimulatory factor 1 and 2 (USF1 and 2), although these transcription factors are apparently not O-GlcNAc modified (12, 123).

The gene encoding OGT (O-linked β-*N*-acetylglucosamine transferase) is essential for embryonic and stem cell development in mammals (42), making it difficult to produce a transgenic knockout model to investigate HBP regulation. Hanover et al. (2005) examined the role of OGT using an *ogt-1* deletion strain of *Caenorhabditis elegans* (42). This strain exhibited no obvious developmental phenotype that was found in homozygous animals and could be used successfully as a model for nutrient-driven insulin resistance. One of the main findings of this model was that homozygous (rat/mouse) lacking *ogt-1* had increased levels of glucose and glycogen, accompanied by a decrease in fat stores (42). This would imply that the HBP was involved in the regulation glycogen synthesis and fatty acid oxidation.

Studies in adipocytes suggest that glucose-induced insulin resistance is caused by impaired translocation of insulin-responsive glucose transporters to the cell membrane (such as GLUT4) and that an increase in glucose flux through the HBP plays a major role in the development of insulin resistance (10-12, 79, 96). There are several observations to suggest that the HBP increases the development of insulin resistance (6, 13, 18, 47, 48, 55, 77, 81, 105, 120). Pre-exposure to glucosamine inhibits basal and insulin-stimulated glucose transport and decreases insulin-stimulated glycogen synthesis in rat muscles without affecting insulin receptor signaling (6, 13, 18, 47, 48, 55, 77, 81, 105, 120). Increasing HBP flux has been shown to alter glucose uptake due to increased O-GlcNAc modification of proteins involved in the regulation of the insulin-signaling cascade, i.e. IRS-1, PI-3 kinase and Akt (31, 90, 132).

A much lower concentration of glucosamine than glucose is required to elicit insulin resistance. The main difference between these two substrates is that glucose is utilised by several pathways where glucosamine is utilised only by HBP. Glutamine or a mixture of amino acids is also an important requirement for the development of glucose-induced insulin resistance of glucose transport in adipocytes (55). When transamidases are added to adipocytes treated with a mixture of amino acids the effect is reversed (55).

Several studies have shown that by increasing the concentration of extracellular glucose and glucosamine, or by increasing glucose uptake by overexpressing glucose transporters (GLUTs) results in insulin resistance (6, 48-50, 62, 77, 78, 80, 94, 105). For example, it was shown that by blocking GFAT with pharmacological agents inhibited glucose-mediated insulin resistance (77). Moreover, other studies found that GFAT overexpression mimicked the effect of treating cells or rats with elevated glucose/glucosamine (18, 22, 25, 80). Also by increasing O-GlcNAc levels in mice and in cell culture genetically or by pharmaceutical intervention, resulted in insulin resistance (5, 14, 42, 81, 90, 120). Together these studies therefore support a strong link between increased HBP flux and the development of insulin resistance/type-2 diabetes.

1.3. Hypothesis

Since the expression of ACCβ is elevated under hyperglycaemic conditions (1-3, 7, 32, 33, 39, 66, 75, 76, 100), ***we hypothesized that increased HBP flux induces cardiac ACCβ gene expression*** **(Figure 4).**

We further propose that since this would result in greater malonyl-CoA production, less fatty acids will be transported into the mitochondria to be oxidised. In the insulin-resistant setting (hyperlipidaemia), failure to oxidise fatty acids is predicted to result in an accumulation of intracellular long chain fatty acids. This, in turn, could result in deleterious effects, for e.g. cell death and contractile dysfunction (68) (Figure 4).

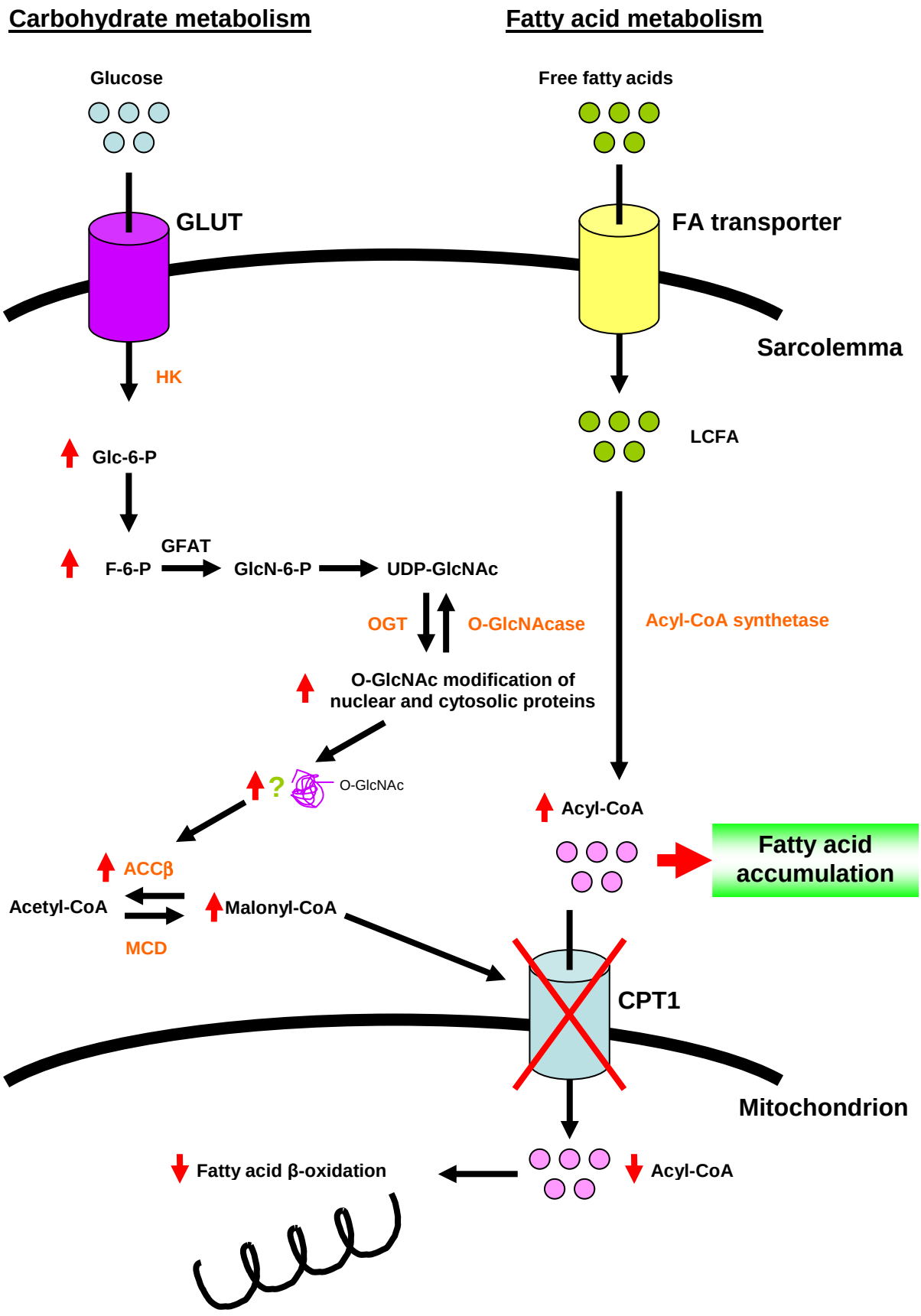

Figure 4: Description of hypothesis.
(HK: hexokinase, OGT: O-linked β-*N*-acetylglucosaminyl transferase, ACCβ: acetyl-coenzyme A carboxylase, MCD: malonyl-CoA decarboxylase, CPT1: carnitine palmitoyl transferase, O-GlcNAcase: β-*N*-acetylglucosaminidase, LCFA: long-chain fatty acid).

1.4. Aims

1. **Transfection** - we will transfect rat cardiac-derived H9c2 myoblasts with a human ACCβ promoter-luciferase construct and a GFAT overexpression construct. The myoblasts will be treated with various inhibitors to test whether the HBP regulates the ACCβ promoter.

2. **Western blotting (*in vitro*)** – Protein extracted from transfected myoblasts will be analysed by Western blotting for the expression of GFAT and O-GlcNAc.

3. **Western blotting (*in vivo*)** – Proteins will be extracted from cardiac tissue from a transgenic mouse model of obesity-induced type-2 diabetes (db/db mouse) and analysed for altered expression of GFAT and O-GlcNAc.

Chapter 2

Methods

2.1. Transfections

2.1.1 Background to principles of the technique

Transfection, i.e. experimental exogenous transfer of DNA into a target cell is a useful method to exploit in order to measure gene promoter activity (Figure 5). Two components are required for a successful transfection. Firstly, a transfection reagent is required that will bind to plasmid DNA to be transferred into the cytosol of cells. For example, for this study Fugene 6 transfection reagent (Roche, Penzberg, Germany) was employed. The second requirement is a plasmid DNA that will be transfected together with the promoter-luciferase construct. The former is constitutively expressed and used to normalise transfection results according to cell number and transfection efficiency.

The gene promoter of interest is bound to a firefly luciferase gene, allowing promoter activity to be measured by the amount of luciferase protein synthesized by the cell. The normalising construct employed for this thesis was pRL-CMV (Promega, Fitchburg, WI, USA). The luciferin protein expressed by the pRL-CMV construct is isolated from *Renilla reniformis*. After transfection, luciferin protein is extracted by cell lysis. Thereafter a substrate called luciferase assay reagent II (LAR II) is added to activate the luciferin protein, resulting in light emission. The latter can be measured using a luminometer. Since the luciferin protein produced by the normalising agent and the promoter construct are different, each can be measured separately from the same sample. Thus, a Dual-Luciferase Reporter Assay Kit

(Promega, Fitchburg, WI, USA) was used where two substrates were added to the same sample, i.e. Luciferase Assay Reagent II (LAR II) (measuring promoter activity) and “Stop and Glo” (neutralizes LAR II substrate and activates the *Renilla* luciferin).

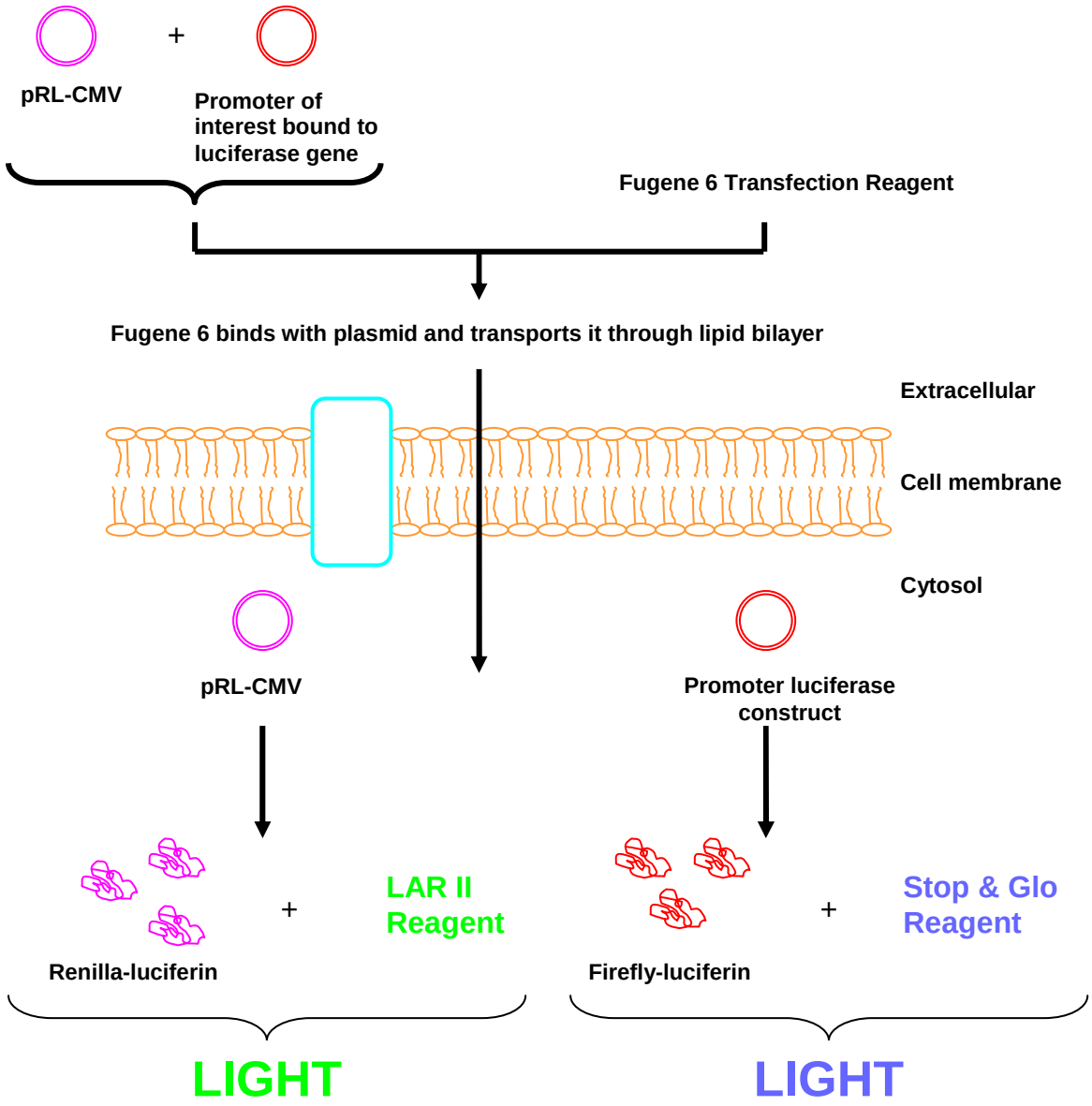

Figure 5: Outline of principles governing gene promoter activity measurements using luciferase assay.
(light: marker of gene promoter activity, LAR II: Luciferase assay reagent II, pRL-CMV: Renilla-luciferase construct).

Transfections were performed as a 5-day experiment (Figure 6). On the first day cells were seeded on 12-well plates. On day 2 cells were transfected, while media of myoblasts was replaced on day 3. This ensured that myoblasts were supplied with sufficient nutrients and also to remove excess transfection reagent. At this stage inhibitors/drugs that were being tested were added (to be discussed later). On day 4, after 24 hours treatment, cells were lysed and the lysate stored at -80°C. The samples were rapidly thawed on day 5 to further enhance cell lysis. Samples were subsequently plated on a 96-well luminometer plate and promoter activity measured (Figure 6).

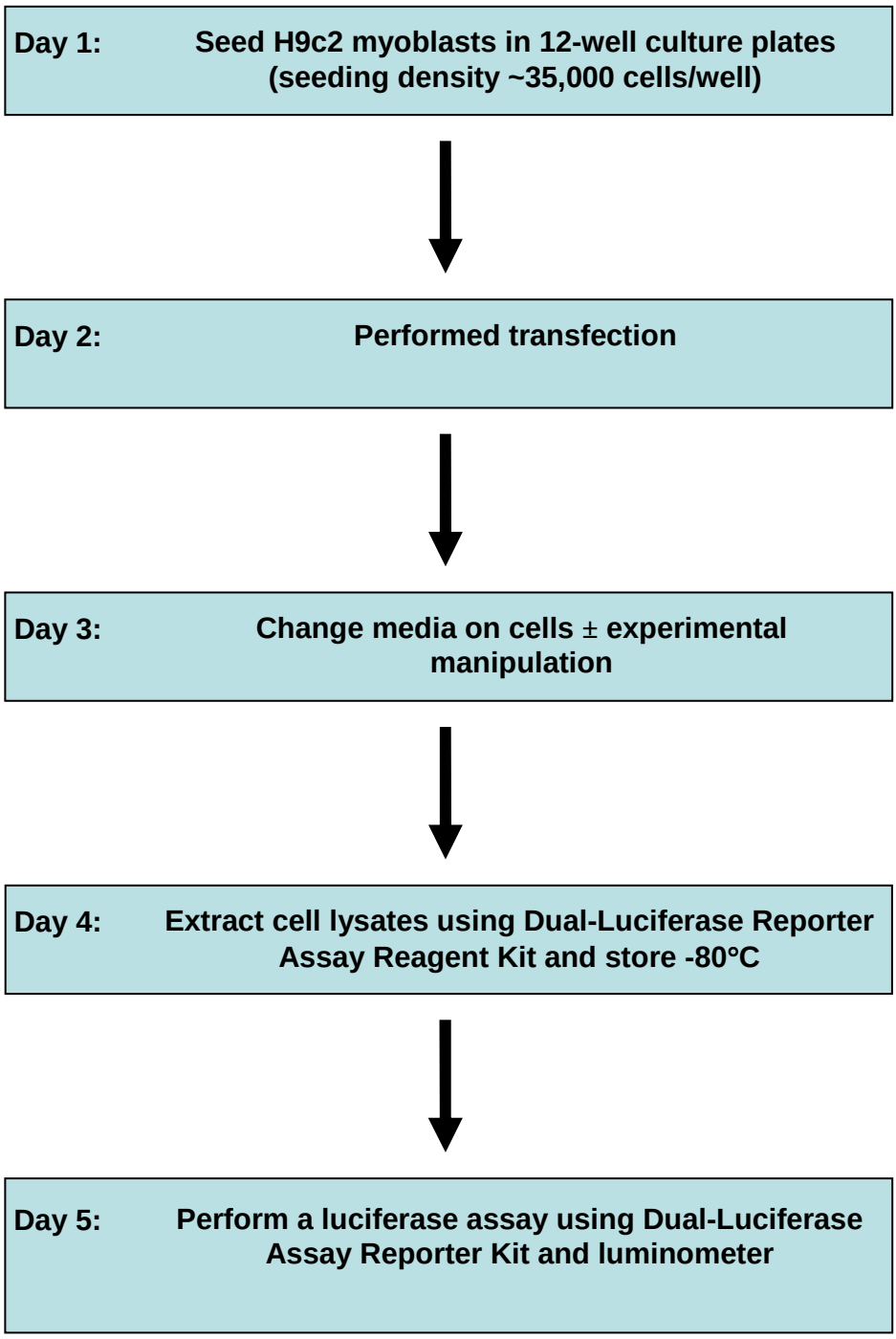

Figure 6: Outline of transfection schedule.

2.1.2. Cell culture

H9c2 rat cardiac-derived myoblasts were chosen for experiments because they are a precursor cell line to cardiomyocytes (19, 38, 91). Precursor cells are also easier to differentiate than terminally differentiated myotubes. H9c2 myoblasts were cultured in T75 culture flasks with Dulbecco's modified Eagle's medium (DMEM) (Highveld, South Africa) with 10% GibCo foetal calf serum (Invitrogen, Carlsbad, CA, USA) and 4 mM GibCo L-glutamine (Invitrogen, Carlsbad, CA, USA). Cells were not allowed to grow to a confluency greater than 80-90% and were cultured for a maximum of 8 passages before growing new cells. We used passages 9-15 for transfection experiments. In our initial optimizing experiments passages 9-15 were used and it was decided to continue using them in order to ensure consistency between results.

Myoblasts were grown as described and plated at 35, 000 cells per well on 12-well culture plates (Greiner, Kremsmünster, Austria) in 1 ml of completed DMEM with 10% foetal calf serum and 4 mM L-glutamine. The cells were incubated for 24 hours at 5% CO_2, 20% O_2 and 95 % humidity at 37°C prior to transfection.

2.1.3. Promoter-luciferase and DNA constructs used for transfection experiments

pGL3-Control (Promega, Madison, WI, USA) was used in all transfection experiments to normalise results according to cell number and transfection efficiency. pGL3-Control is a plasmid constitutively expressing luciferase from an SV40 promoter. pGL3-Basic is a plasmid lacking a promoter and therefore expresses only baseline levels of luciferase. The latter was used to normalise the total amount of DNA used per transfection to ensure comparable transfection efficiency between experiments. The total amount of DNA transfected for each experiment was 0.75 µg, and pGL3- Basic was used to make up the remaining DNA needed. H9c2 myoblasts were transiently transfected with a 1,317 bp human ACCβ promoter-luciferase reporter construct (pPIIβ-1,317) previously described (Makaula et al., 2006) (75). 0.25 µg of pPIIβ-1,317 was transfected ± 0.25 µg of a human pcDNA3-GFAT expression vector (123). Two dominant negative constructs, i.e. pcDNA3-GFAT577 and pcDNA3-GFAT667 were also employed in this study (123). Both dominant negative constructs were separately transfected with pPIIβ-1,317 and GFAT. There is a great amount of sequence homology between the rat and human isoforms of GFAT (91%) and ACCβ (90%) and therefore it is unlikely that this would represent a problem when expressing human constructs in a rat cardiac-derived cell line.

Description of plasmid constructs:

1. pcDNA3-GFAT (see Figure 7) contains a full-length human GFAT cDNA generated by RT-PCR and cloned into the expression vector pcDNA3.1 (see Figure 8) (Invitrogen, Inchinnan, Scotland). The PCR product was verified by sequencing and shows identity to human GFAT (also known as GFAT1 = glutamine:fructose-6-phosphate transaminase 1, GenBank accession number M90516). This construct was kindly donated to us by Dr. Cora Weigert (University of Tübingen, Germany).

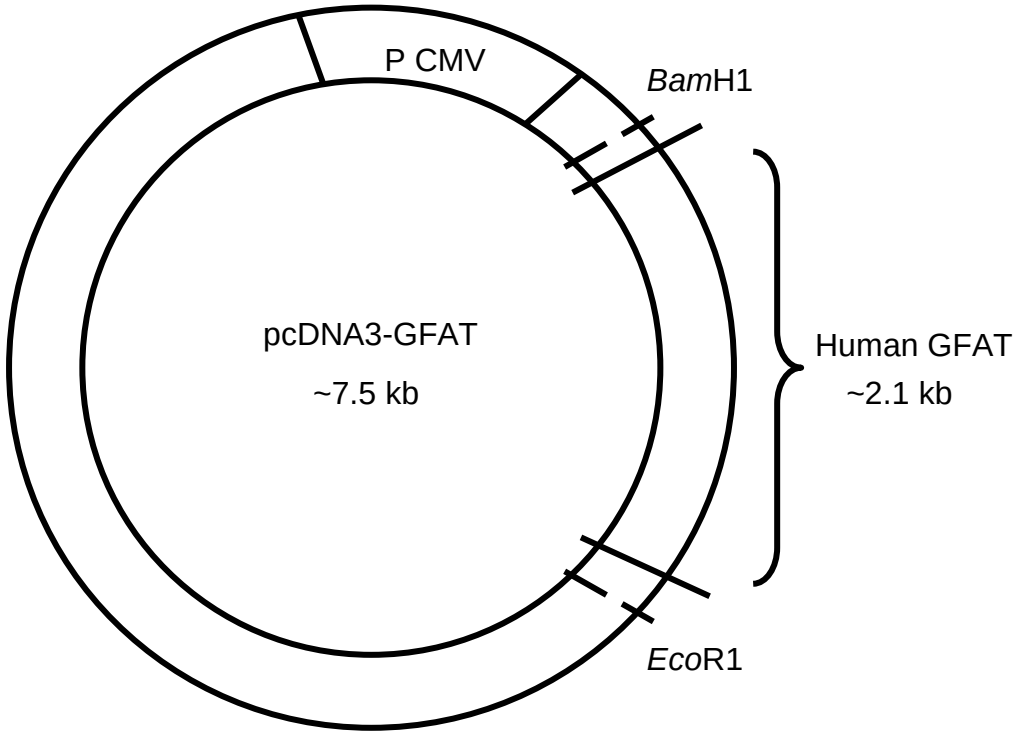

Figure 7: Sketch of human GFAT gene cloned into pcDNA3.1 vector (123). (from Weigert et al., 2003) (pRL-CMV: Vector, GFAT: glutamine:fructose-6-phosphate amidotransferase, *Eco*R1 and *Bam*H1 are restriction splice sites).

2. pcDNA3-GFAT/577 contains human GFAT1 cloned into the pcDNA3.1 vector but with histidine 577 mutated to alanine, resulting in the complete loss of GFAT enzyme activity (Weigert et al., 2003).

3. pcDNA3-GFAT/677 contains human GFAT1 cloned into the pcDNA3.1 vector but with lysine 667 mutated to alanine, leading to complete loss of GFAT enzyme activity (Weigert et al., 2003).

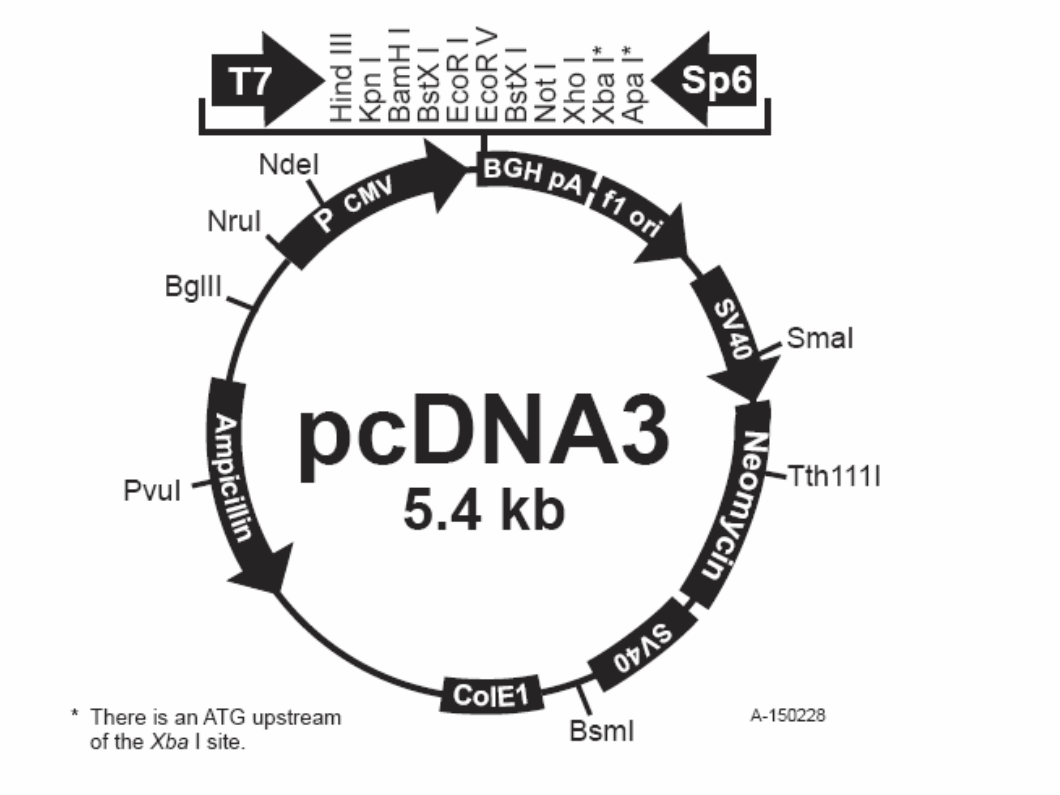

Figure 8: Diagram of pcDNA3 vector (from brochure supplied by Invitrogen, Carlsbad, CA, USA)**.**

4. pPIIβ-1,317 is a full-length human ACCβ promoter reporter luciferase construct that contains 4 E-boxes (CANNTG) (Figure 9) (Makaula et al, 2006).

ACCβ promoter region = 1,317 bp

Four ''E-boxes'' identified (E1-E4): important regulatory elements for transcription factors such as upstream stimulatory factor (USF)

Figure 9: Diagram of pPIIβ-1,317 construct (modified from Makaula et al., 2006).
(E1: Ebox 1, E2: Ebox 2, E3: Ebox 3, E4: Ebox 4, pPIIβ-1317: human ACCβ pomoter-reporter construct).

5. TransLucent USF Reporter Vector (USF-L) contains promoter recognition sites for both upstream stimulatory factor 1 (USF1) and upstream stimulatory factor 2 (USF2) cloned into a pTransLucent Vector (catalog number LROO86, Panomics, Redwood City, USA) (Figure 10).

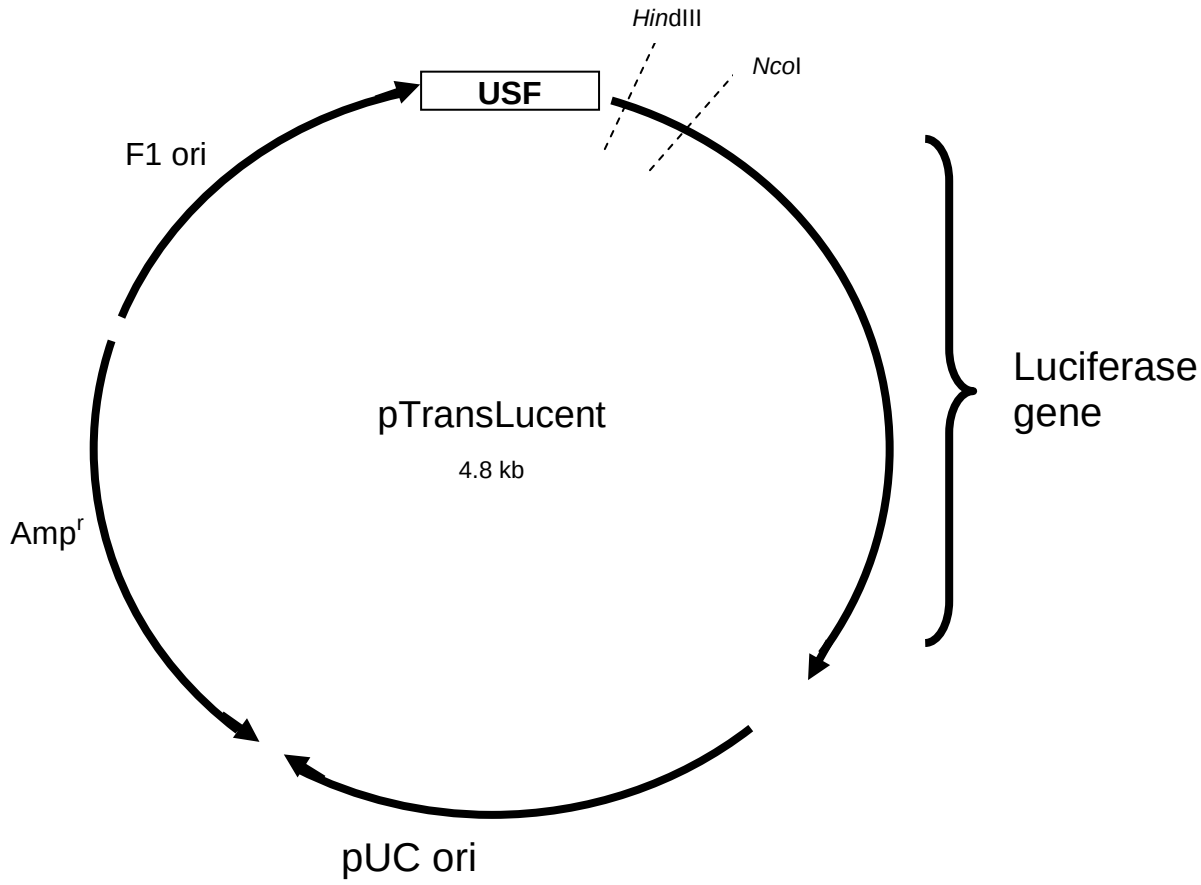

Figure 10: Diagram of pTransLucent construct. (Panomics, Redwood City, USA). (*Hin*dIII and *Nco*I are restriction sites where the USF promoter is cloned).

2.1.4. Preparation of plasmid DNA

Each expression vector was amplified in *Escherichia coli* cultures (JM109 competent cells, Promega, Madison, WI, USA) and extracted using the Qiagen® Plasmid Purification Maxi Kit (Qiagen, Invitrogen, Carlsbad, CA, USA). Purified DNA was quantified using a spectrophotometer (wavelengths of 260 nm and 280 nm) and its quality checked by restriction enzyme analysis. The DNA was electrophoresed on a 1% agarose gel to check for the quality of the DNA.

2.1.5. Transfection procedures

On Day 2 of transfection experiments the cells were transfected with the DNA of interest (Figure 6). Transfections were performed in triplicate for each experiment and repeated to generate the necessary numbers for statistical analysis. First, a stock solution of pGL3-Control DNA (pRL-CMV) was made in media concentration of 10 ng/ml (see step 1 of Figure 11). The media contained DMEM and 4 mM L-glutamine. The stock solution was aliquoted into separate microfuge tubes to a final volume of 165 µl for every transfection experiment (consisting of three replicates for each experiment) (see step 2 of Figure 11). DNA was aliquoted into its respective microfuge tubes with pGL3-Basic making up the total DNA mass to 0.75 µg (step 3 of Figure 11).

A second stock solution was then prepared with an equal volume of media containing Fugene 6 Transfection Reagent (Roche, Penzberg, Germany). Here, a 2:1 ratio of Fugene 6: DNA (with DMEM and 4 mM L-glutamine) was used. 165 µl of the Fugene 6 solution was then added to each of the microfuge tubes containing DNA and incubated at room temperature for 15 minutes (steps 4, 5 of Figure 11).

Meanwhile, 0.9 ml of fresh medium (containing DMEM, 10% FCS and 4 mM L-glutamine) was added to the H9c2 cells before the transfection. The final volume of the DNA/Fugene 6 cocktail therefore equalled 330 µl in each microfuge tube for each transfection experiment.

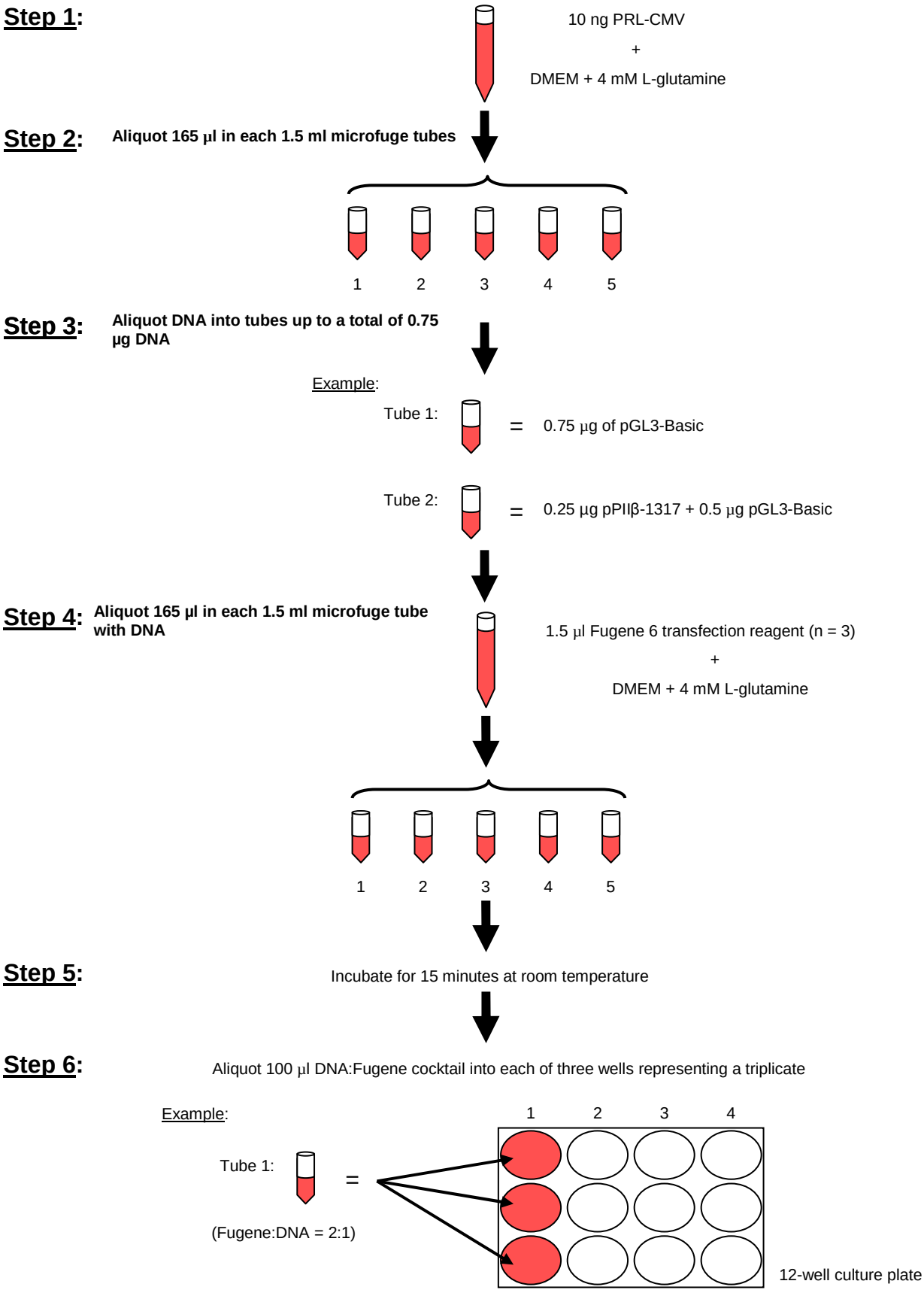

Figure 11: Outline of day 2 transfection procedure.
(n: number of samples, DMEM: Dulbecco's modified Eagle's medium, pGL3-Basic : vector, PRL-CMV: Renilla luciferase construct).

The DNA/Fugene 6 solution was added to the H9c2 myoblasts (100 µl per well to make a final volume of 1 ml per well). The solutions were applied in triplicate (step 6 of Figure 11). The plates were gently rocked and then incubated at 37℃ for 24 hours.

After 24 hours the media on the cells was changed. During this media change various drugs of interest were added to cells. We employed the following agents: 0.1 mM, 1 mM and 2 mM alloxan (Sigma-Aldrich, St. Louis, Missouri), 40 µM and 80 µM azaserine (Sigma-Aldrich, St. Louis, Missouri), 40 µM and 80 µM 6-Diazo-5-oxo-L-norleucine (DON) (Sigma-Aldrich, St. Louis, Missouri) and 5 mM and 10 mM streptozotocin (STZ) (Sigma-Aldrich, St. Louis, Missouri). Twenty-four hours later cells were lysed, protein extracted and expression of luciferase measured using the Glomax luminometer (Promega, Fitchburg, WI, USA).

The protocol and reagents used were as stipulated in the manual of the Dual-Luciferase Reporter Assay Kit (Promega, Fitchburg, WI, USA). First the cells were washed with phosphate buffer saline and then 200 µl of Passive Lysis Buffer (Promega, Fitchburg, WI, USA) was added to each well. The 12-well plate was then incubated on a shaker at room temperature for 15 minutes. The lysis buffer and cells from each well were transferred to microfuge tubes. A separate microfuge tube was used for each well of the 12-well plate. The microfuge tubes carrying the cells and lysis buffer were stored at -80°C (Figure 12). On Day 5 the lysate was thawed in water and vortexed. The microfuge tubes were centrifuged at 12,000 rpm at 4°C for 2 minutes with a ALC multispeed refrigerated centrifuge PK 121R (Intergrated Services, New

Jersey, USA). 10 µl of each sample was aliquoted into a separate well on a 96-well luminometer plate (Amersham, Buckinghamshire, UK).

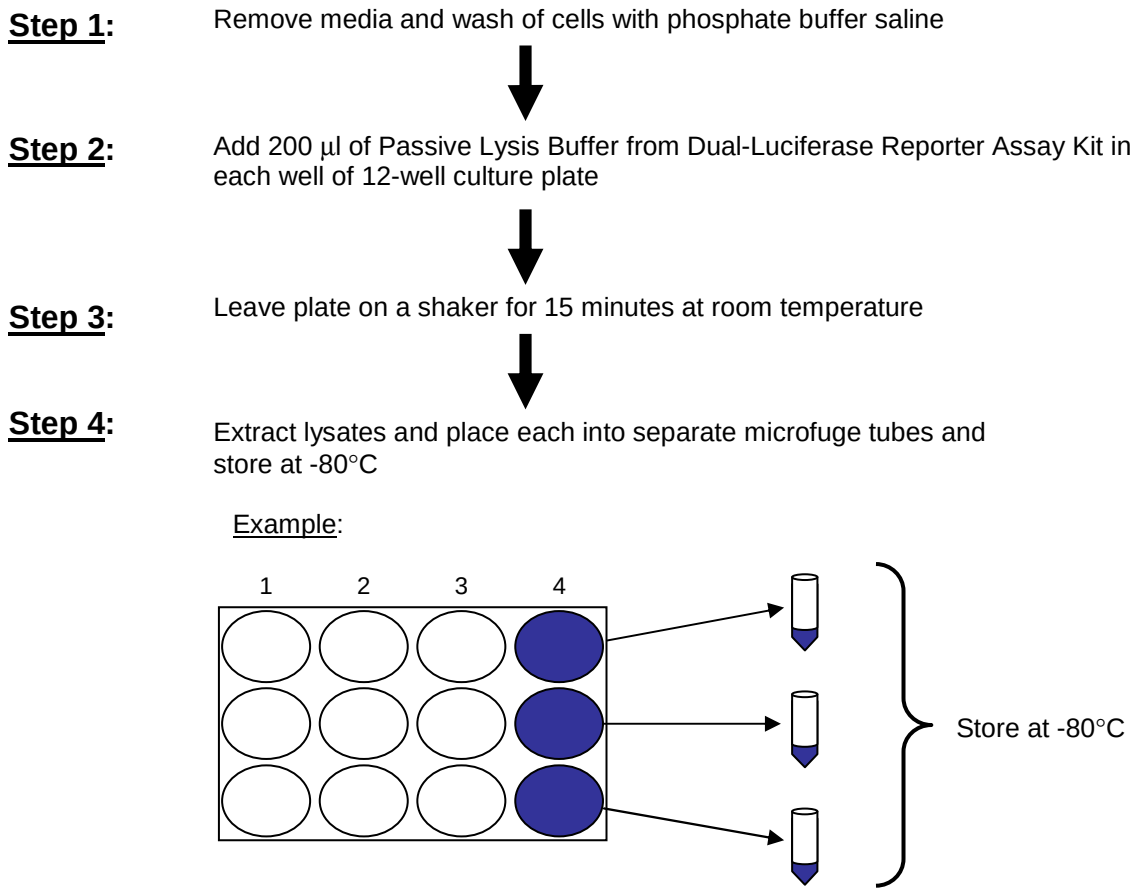

Figure 12: Outline of day 4 lysate extraction.

Two reagents had to be prepared. Reagent 1 contained Luciferase Assay Reagent II (LAR II) and reagent 2 Stop and Glo reagent (Figure 13). Both reagents were provided with the Dual-Luciferase Reporter Assay Kit (Promega, Fitchburg, WI, USA). The luminometer plate, together with the two reagents, was placed in the luminometer. The luminometer was set up to add 50 µl of LAR II, delay for 2 seconds and then take a reading for 8 seconds. This gave a measurement for human ACCβ promoter (pPIIβ-1,317) activity. The luminometer then added “Stop and Glo” to the same well and delayed for 2 seconds before measuring the light released (for another 8 seconds). This yielded the measurement for the Renilla construct (pRL-CMV) of the same sample. The process was repeated for each well, providing two readings for each sample (Figure 13).

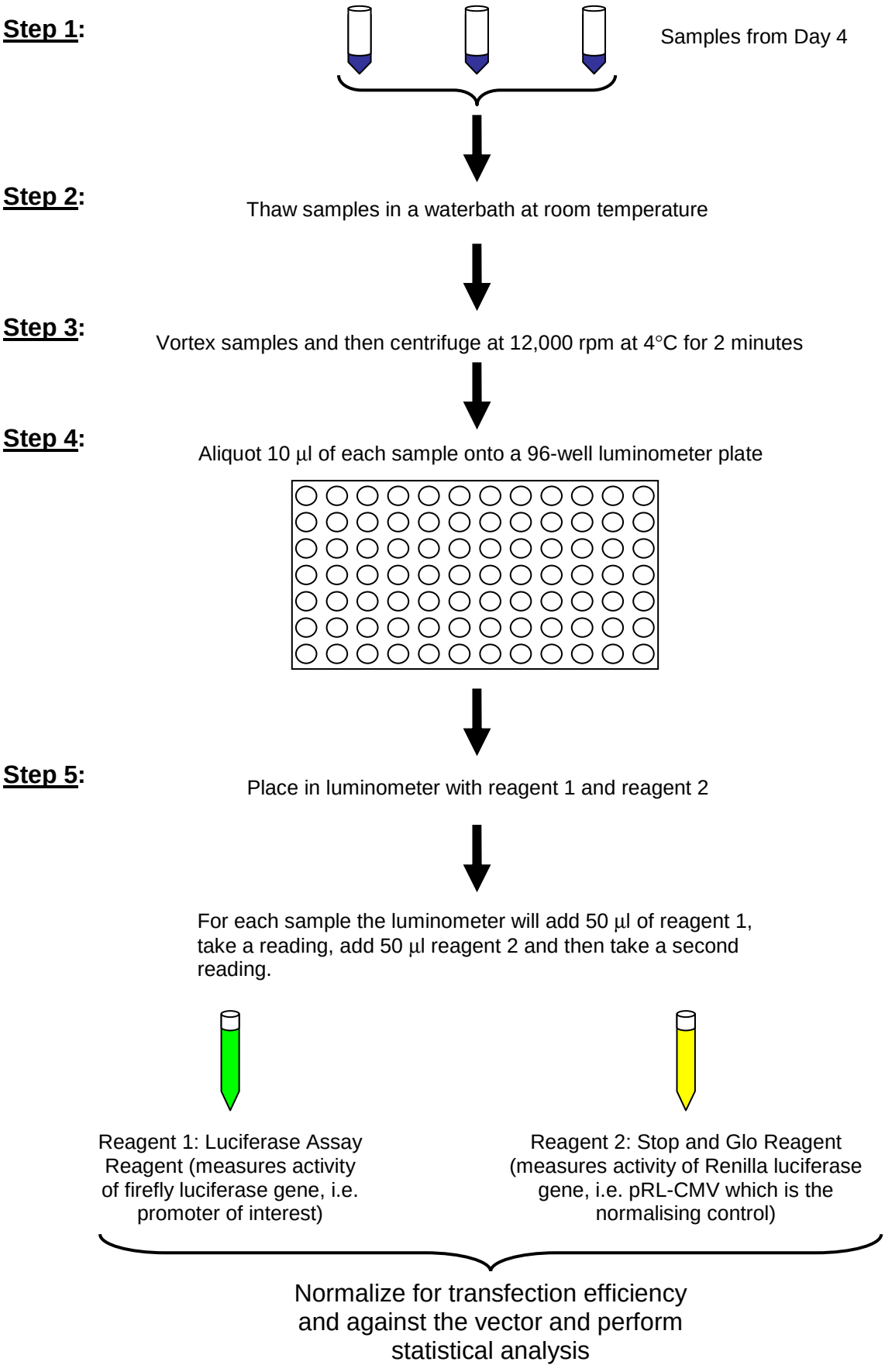

Figure 13: Performing the luciferase assay on day 5.

2.1.6. Statistical analyses of transfection results

Luminometer firefly readings for each experiment were normalised against its respective Renilla luminometer reading by dividing the firefly reading by its renilla reading. Each experiment was performed in triplicate each time a transfection was carried out. Each replicate of an experiment was added together and then divided by 3 to give a mean value for each experiment. This provided a mean value for each experiment that was normalised according to transfection efficiency and cell number. To eliminate any vector effects (i.e. in which the construct were cloned) on the experiment, each of the mean values were divided by the vector's mean value.

The transfection experiments were repeated numerous times to provide a larger number of replicates for each experiment. Measurements from all the same experiments were combined and Graphpad Instat version 3.01 (GraphPad Software Inc., San Diego CA) used to perform statistical analyses of these values. First the mean and standard error of the mean and standard deviation was calculated. A 95% confidence interval was also calculated. Replicates of an experiment that were outside the 95% confidence interval or were not within two standard errors of the mean were discarded. The remaining replicates were used to plot a graph. Student-Newman statistical test was used to see if there were in significant differences between controls and the experiments in each set of experiments. Values $p< 0.05$ were taken as being significant.

2.2. Protein and RNA extraction from transfected cells

On day 4 of transfection experiments, protein and RNA were extracted from H9c2 myoblasts using an Allprep RNA/Protein extraction kit (Qiagen, Invitrogen, Carlsbad, CA, USA). This was done in duplicate so that a luciferase assay could be performed to confirm that transfection experiments were indeed successful. Protein extracted from these cells was used in Western blotting experiments, while the RNA was stored for future real-time PCR experiments.

2.3. Western blotting

2.3.1. Sample preparation and quantification of protein from cells

The protein extracted using the Allprep RNA/Protein extraction Kit was quantified using the Qubit flourometer (Invitrogen, Carlsbad, CA, USA). Protein was prepared with an equal volume of sample buffer and boiled for 5 minutes, centrifuged at 14,000 rpm for 5 seconds before loading onto a SDS-polyacrylamide gel for electrophoresis.

2.3.2. Tissue biopsies acquired from db/db transgenic mouse model of type-2 diabetes

Previously collected heart tissues from 20-week-old male and female db/db mouse and matching controls (db/+) were used. This mouse has a point mutation in the leptin receptor gene and gains weight with age (15). They also develop insulin resistance and hyperglycaemia, eventually progressing to type-2 diabetes. The symptoms of type 2 diabetes are similar to that observed in the human condition making this a good model to explore my hypothesis in an *in vivo* setting. We used heterozygous (db/+) instead of homozygous (+/+) as controls because of a lack of animal supply.

2.3.3. Sample preparation and quantification of protein from heart tissues

Protein was extracted from male and female db/db mouse and heterozygous mouse heart muscle tissue biopsies and stored in RIPA buffer (refer to Appendix 1 for extraction method). Total protein was quantified using the Bradford method for protein determination (see Appendix 2 for Bradford method). 50 µg of sample was then added to an equal volume of sample buffer and boiled for 5 minutes. The samples were then electrophoresed on a SDS-polyacrylamide gel.

2.3.4. Gel analysis

Protein extracts were electrophoresed on a 10% SDS-polyacrylamide gel with a 4% stacking gel at 200 V for 1 hour. 10 µl of a protein marker (BioRAD precision Plus protein standard cat. # 161-0374, Bio-RAD Laboratories, California, USA) was used in lane 1 of gels. The amount of protein loaded per well was 50 µg for each sample. The protein was then transferred to a PVDF membrane using a semi-dry transfer apparatus (Bio-RAD Laboratories, California, USA) for 1 hour (See Appendix 3 for electrotransfer procedure).

The membranes were used to probe for three proteins of interest:

1) O-GlcNAc was detected using an O-GlcNAc Western Blot Detection Kit (Pierce, catalogue number 24565, Rockford, Illinois) (Refer to Appendix 4 for complete protocol).

2) GFAT (Refer to Appendix 5 for the complete protocol). The GFAT antibody was kindly donated by Dr. Cora Weigert (University of Tübingen, Germany).

3) β-actin (Cell Signaling, Danvers, MA, USA) was also employed to check for equal protein loading (Refer to Appendix 6 for protocol).

2.3.5. Analysis of Western blot results

Results from western blots were analysed by densitometry. For the *in vivo* studies db/db protein extracts were probed with O-GlcNAc or GFAT antibody, reprobed with β-actin (Cell Signaling, Danvers, MA, USA) and then densitometry was performed. The densitometry was performed by scanning the blots with an HP Scanjet 3500c scanner (Hewlett Packard, Palo Alto CA) and densitometry was performed on the scanned pictures using Un-Scan-It Gel version 5.1 (Silk Software, Orem, UT). The densitometry value for a sample was normalised against its β-actin densitometry value. Then all the normalised densitometry values from db/db were pooled together (likewise for db/+). The combined protein expression for db/+ was compared to that of db/db using appropriate statistical analyses to evaluate if there was a significant change in protein expression.

Chapter 3

Results

3.1. Transfections

Before investigating our hypothesis, my initial experiments were focused on optimising the transfection procedure for H9c2 myoblasts. Here myoblasts were transfected with different concentrations of the ACCβ promoter-luciferase reporter construct (pPIIβ-1317/+65) ± different concentrations of GFAT expression vector ± different concentrations of dominant negative GFAT/577 or GFAT/677 constructs. After considerable effort, I eventually was in a position to select optimal DNA concentrations for use in transfection experiments (Figure 14). For these initial experiments a total of 1 µg of DNA per experiment was employed. The results obtained showed inconsistency. The transfection procedure was then re-optimised. Thus, for the experiments which followed we used 0.75 µg of DNA per experiment; however the Fugene 6 to DNA ratio remained at 2:1.

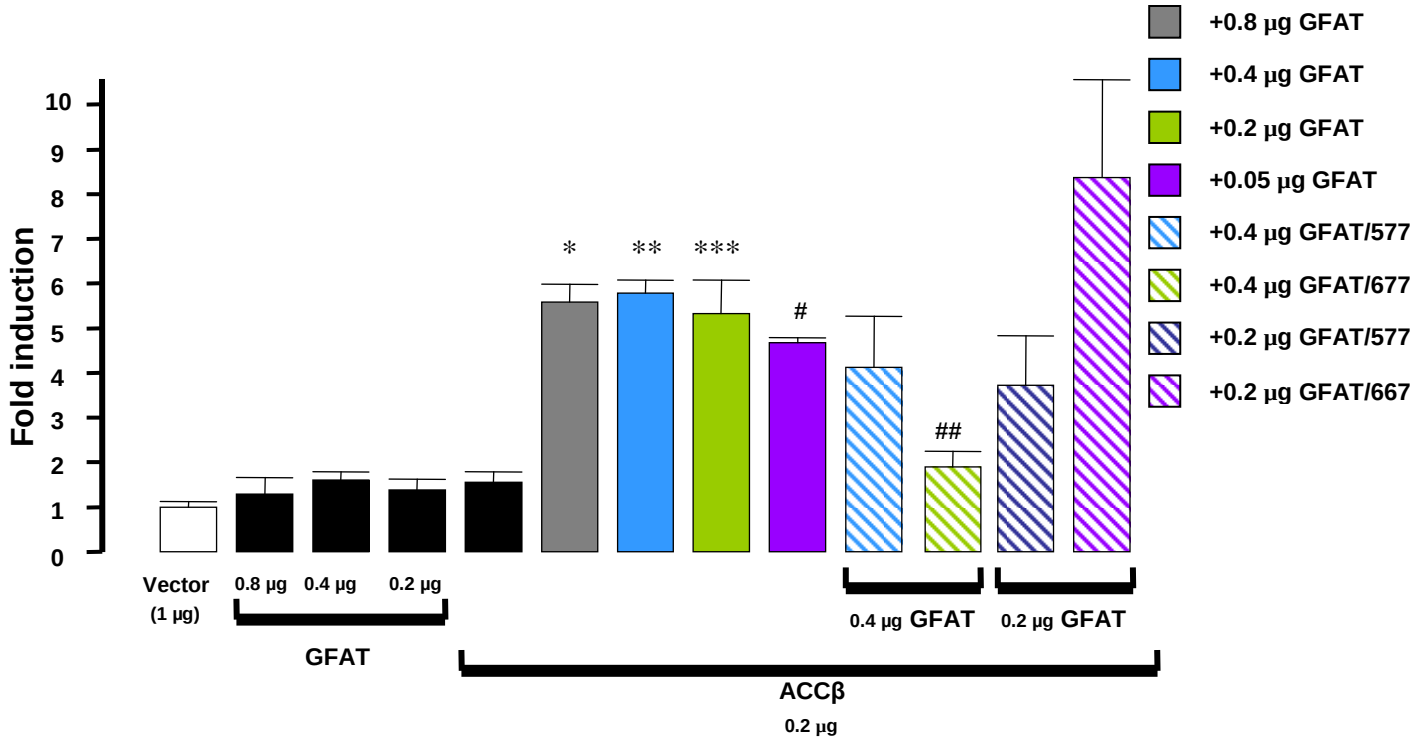

Figure 14: Results of pilot co-transfection experiments performed with ACCβ promoter, GFAT and dominant negative constructs (GFAT/577 and GFAT/667).
(∗ p<0.001 vs. ACCβ [n=9], ∗∗ p<0.05 vs. ACCβ [n=9], ∗∗∗ p<0.01 vs. ACCβ [n=9], # p<0.01 vs. ACCβ [n=9], ## p<0.001 vs. ACCβ+ 0.4 µg GFAT [n=5]. Vector: pRL-CMV, ACCβ: pPIIβ-1317/+65, GFAT: glutamine:fructose-6-phosphate amidotransferase).

After establishing and optimising the transfection procedure I next proceeded to investigate my hypothesis. To ensure that results were statistically relevant experiments were repeated several times (at least an n=6).

I began by transiently transfecting H9c2 myoblasts with the human ACCβ promoter-luciferase reporter construct (pPIIβ-1317/+65) ± a GFAT expression vector ± dominant negative GFAT/577 or GFAT/677 constructs. The results showed that GFAT overexpression induced ACCβ gene promoter activity by 75 ± 23% ($p<0.001$, n=6). Co-transfection with either GFAT/577 or GFAT/667 constructs resulted in marked attenuation of this induction (Figure 15).

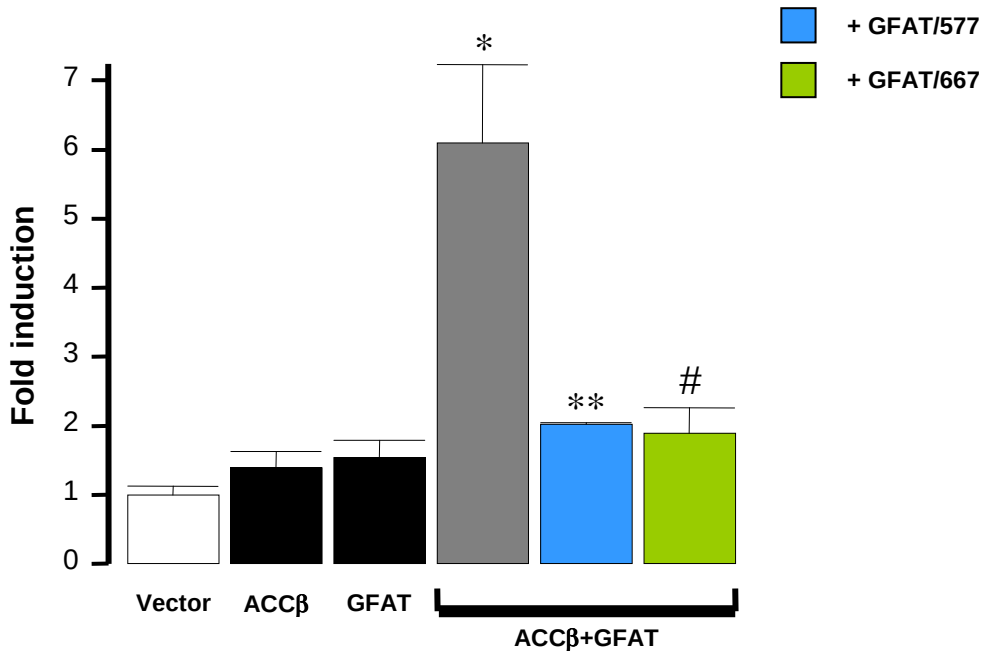

Figure 15: GFAT overexpression induces ACCβ gene promoter activity.
(∗ $p<0.001$ vs. ACCβ [n=9], ∗∗ $p<0.001$ vs. ACCβ+GFAT [n=6], # $p<0.001$ vs. ACCβ+GFAT [n=6]. Vector: pRL-CMV, ACCβ: pPIIβ-1317/+65, GFAT: glutamine:fructose-6-phosphate amidotransferase).

To assess the extent of GFAT regulation on ACCβ gene promoter activation, H9c2 myoblasts were treated with varying doses of L-glutamine (0 mM, 4 mM and 8 mM) a substrate for the hexosamine biosynthetic pathway (HBP). Here, glutamine induced ACCβ promoter activity in a dose-dependent manner (Figure 16). There was no significant change in ACCβ promoter activity in the absence of GFAT (Figure 16).

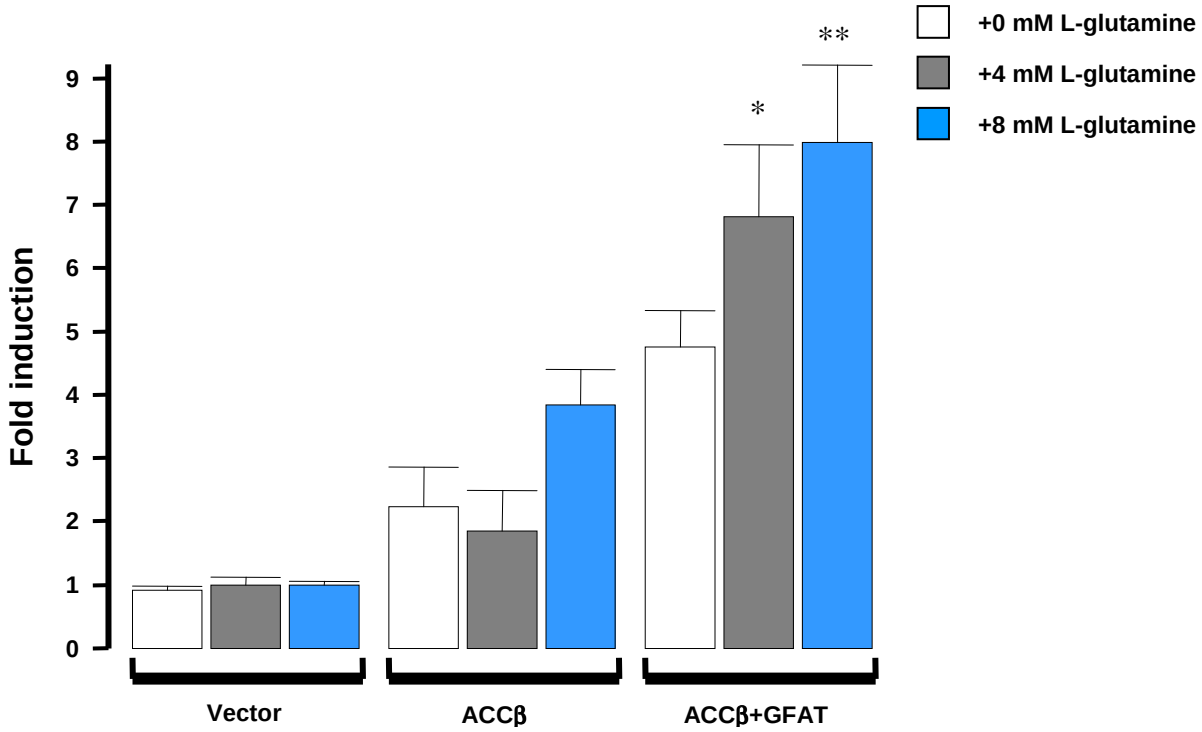

Figure 16: Glutamine induces ACCβ promoter activity in a dose-dependent manner.
(* p<0.05 vs. ACCβ + GFAT 0 mM L-Glutamine [n=7], ** p<0.01 vs. ACCβ+GFAT + 0 mM L-Glutamine [n=7]. Vector: pRL-CMV, ACCβ: pPIIβ-1317/+65, GFAT: glutamine:fructose-6-phosphate amidotransferase).

Since GFAT-induced ACCβ promoter activity was inhibited by dominant negative constructs, I next performed additional comfirmatory experiments by pharmacological inhibition of GFAT. Two inhibitors of GFAT were used, i.e. 6-Diazo-5-oxo-L-norleucine (DON) and azaserine (Figure 17).

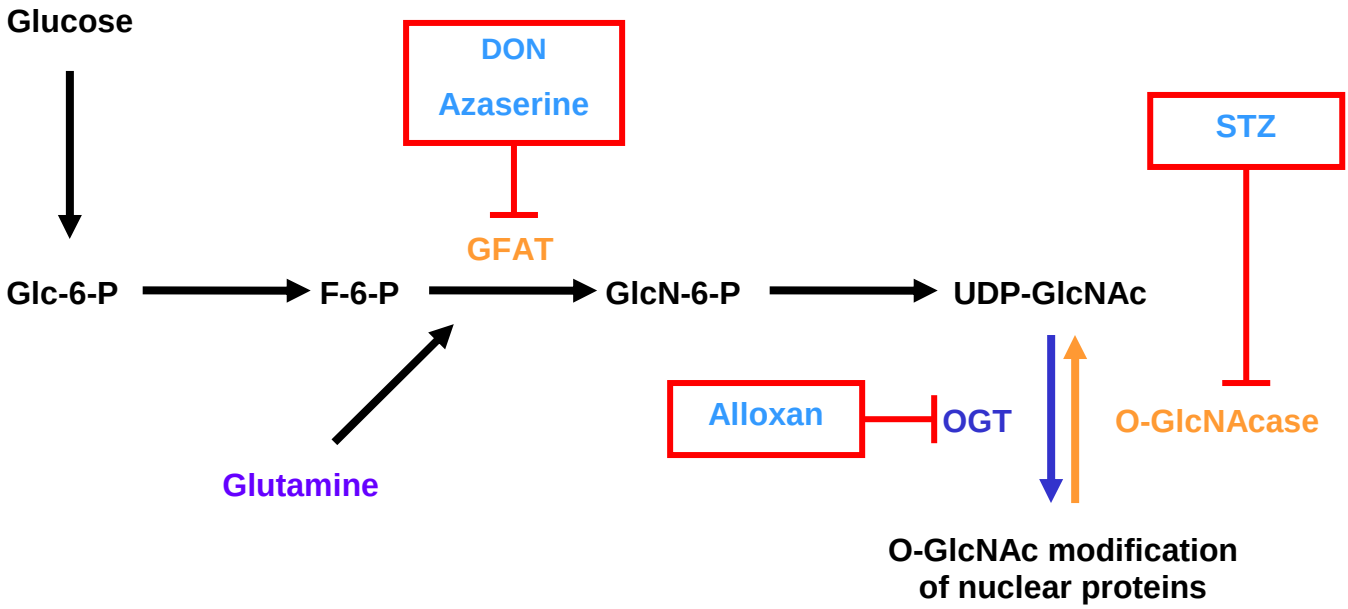

Figure 17: Description of inhibitors of HBP and where they operate.
Glc-6-P: glucose-6-phosphate, F-6-P: fructose-6-phospahate, GlcN-6-P: *N*-glucosamine-6-phosphate, UDP-GlcNAc: uridine diphospho-*N*-acetylglucosamine, OGT: O-linked β-*N*-acetylglucosamine transferase, GFAT: glutamine:fructose-6-phosphate amidotransferase, O-GlcNAc: O-linked *N*-acetylglucosamine

Two concentrations of DON were used (40 µM and 80 µM) to determine the effectiveness of DON inhibition (Figure 18). It was suggested in the literature that 40 µM of DON would be a physiologically relevant dose to achieve the required effect. Since the cell line used in this study was different to published data the dose was also doubled to 80 µM in case the 40 µM dose failed to inhibit GFAT.

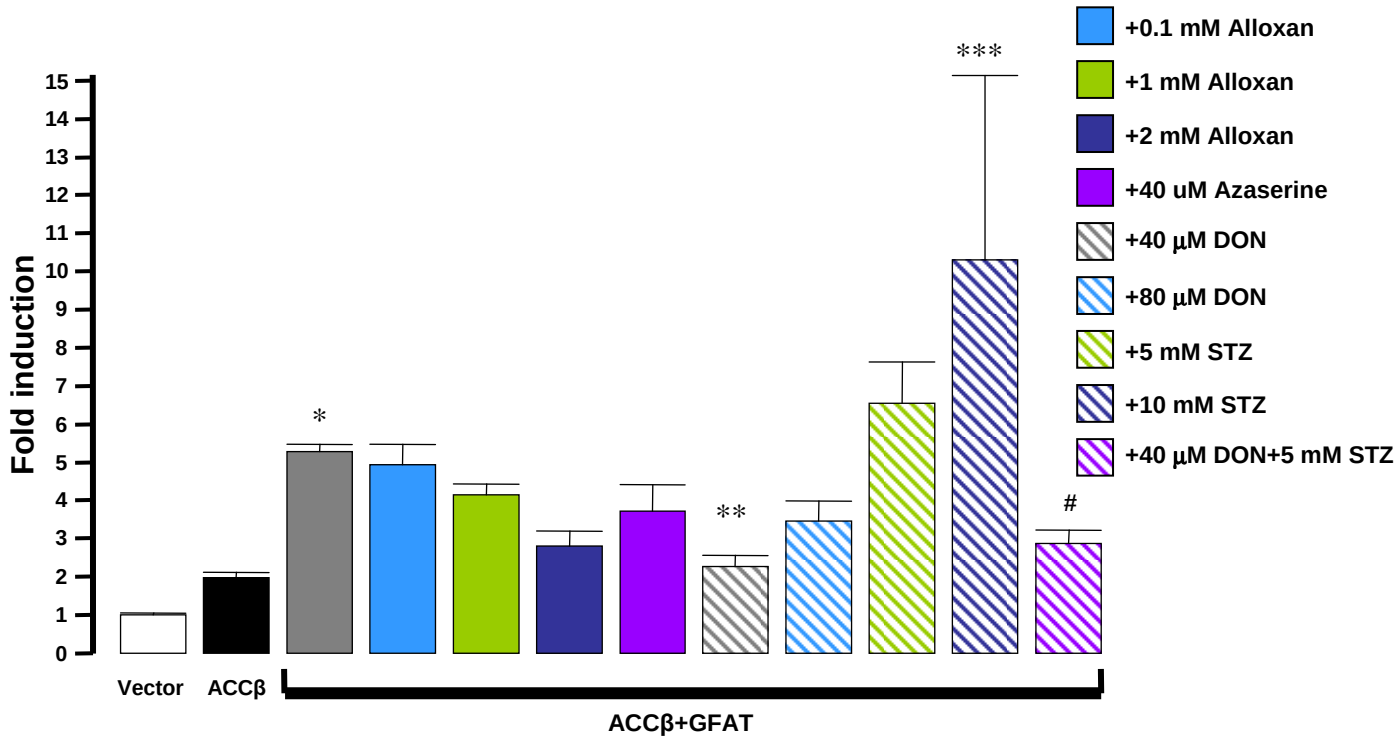

Figure 18: Results of co-transfection experiments performed with ACCβ, GFAT and different concentrations of inhibitors of HBP.

(∗ p<0.05 vs. ACCβ [n=9], ∗∗ p<0.05 vs. ACCβ+GFAT [n=10], ∗∗∗ p<0.01 vs. ACCβ+GFAT [n=9], # p<0.01 vs. ACCβ+GFAT+STZ [n=7]. Vector: pRL-CMV, ACCβ: pPIIβ-1317/+65, GFAT: glutamine:fructose-6-phosphate amidotransferase, DON: 6-Diazo-5-oxo-L-norleucine, STZ: Streptozotocin).

Since both the 40 µM and 80 µM concentrations worked equally well (Figure 19) we continued by using the 40 µM dose as it was more cost effective.

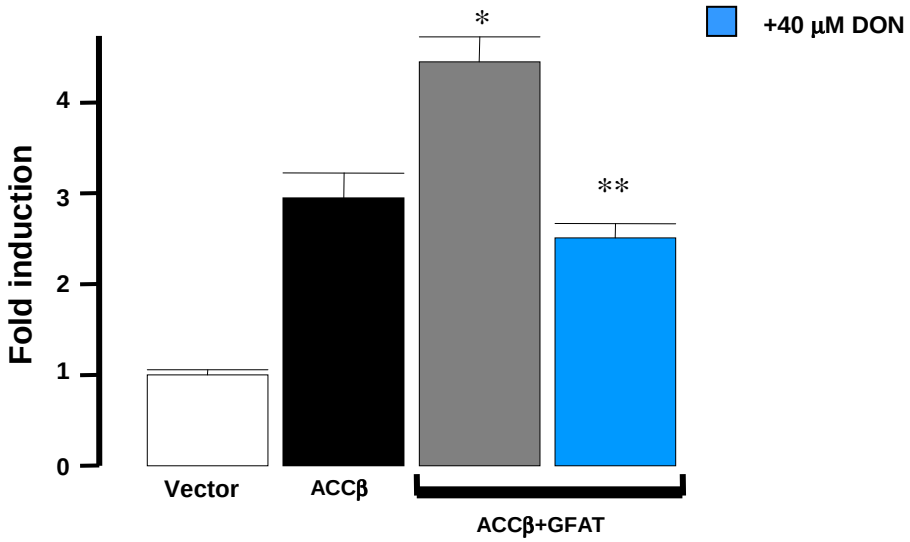

Figure 19: Pharmacological inhibition of GFAT abolishes ACCβ promoter induction.
(* p<0.001 vs. ACCβ [n=35], ** p<0.001 vs. ACCβ+GFAT [n=25]. Vector: pRL-CMV, ACCβ: pPIIβ-1317/+65, GFAT: glutamine:fructose-6-phosphate amidotransferase, DON: 6-Diazo-5-oxo-L-norleucine).

Two concentrations of azaserine were tested (40 µM and 80 µM) (Figure 19). Again, as before we employed the 40 µM dose because of cost effectiveness. Azaserine markedly blunted GFAT-induced ACCβ promoter activity (Figure 20). Therefore both the dominant negative and pharmaceutical data substantially strengthen our hypothesis that the HBP regulates ACCβ promoter activity.

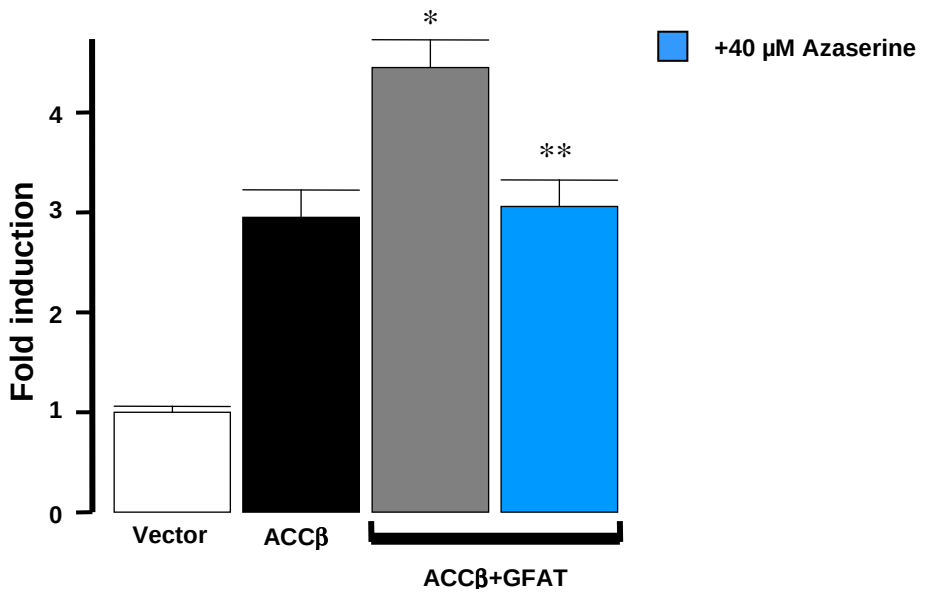

Figure 20: Pharmacological inhibition of GFAT attenuates ACCβ promoter induction.
(∗ p<0.001 vs. ACCβ [n=35], ∗∗ p<0.001 vs. ACCβ+GFAT [n=24]. Vector: pRL-CMV, ACCβ: pPIIβ-1317/+65, GFAT: glutamine:fructose-6-phosphate amidotransferase).

Additional pharmaceutical agents were next employed to further examine the regulation of ACCβ promoter activity by downstream targets of the HBP. Here H9c2 myoblasts were treated with various concentrations of alloxan (0.1 mM, 1 mM and 2 mM), an inhibitor of O-linked β-*N*-acetylglucosaminyl transferase (OGT) (Figure 17). The results show that increasing concentrations of alloxan result in a corresponding decrease of ACCβ promoter activity in response to GFAT overexpression (Figure 21). Moreover, at the 2 mM alloxan concentration there was a significant reduction in ACCβ promoter activity (Figure 21).

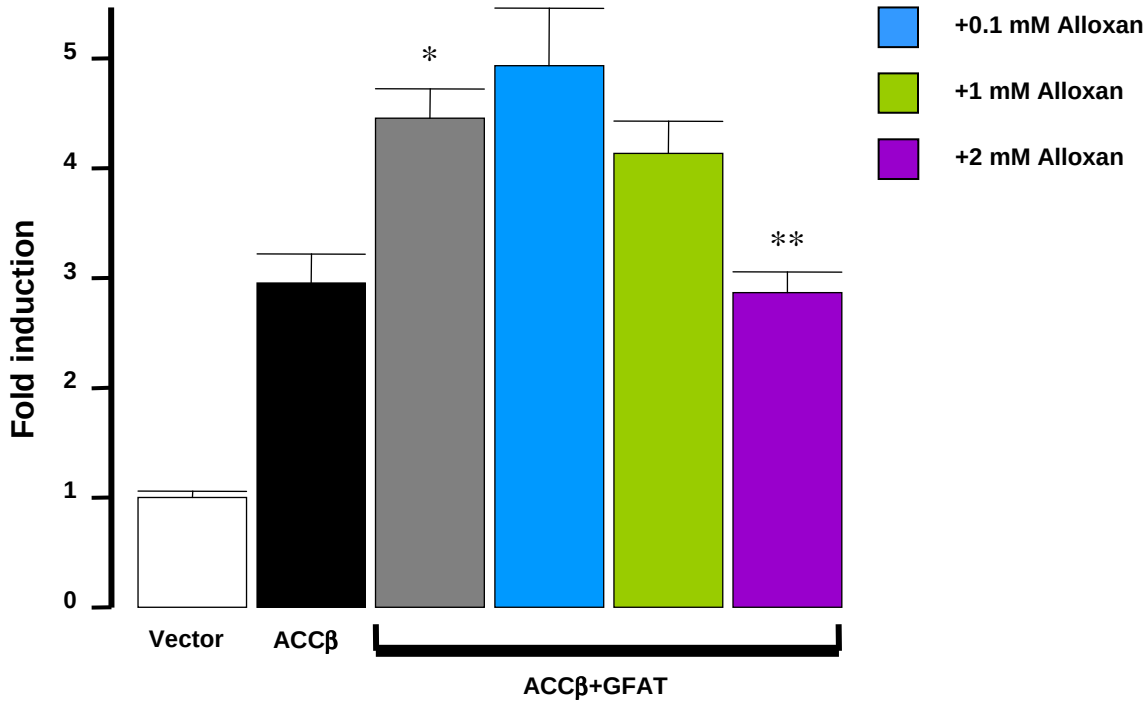

Figure 21: Pharmacological inhibition of OGT blunts ACCβ promoter induction.
(∗ p<0.001 vs. ACCβ [n=35], ∗∗ p<0.001 vs. ACCβ+GFAT [n=16]. Vector: pRL-CMV, ACCβ: pPIIβ-1317/+65, GFAT: glutamine:fructose-6-phosphate amidotransferase).

A second pharmacologic inhibitor, i.e. streptozotocin (STZ), an inhibitor of β-*N*-acetylglucosaminidase (O-GlcNAcase) was used to investigate downstream targets of the HBP on the regulation of ACCβ promoter activity (Figure 17). Thus I expected to observe an increase in ACCβ promoter activity in this instance. Two concentrations of STZ were used (5 mM and 10 mM) in preliminary testing, and we thereafter employed the 5 mM dose (Figure 19). Interestingly, these results show that STZ further enhanced GFAT-induced ACCβ promoter activity (Figure 22).

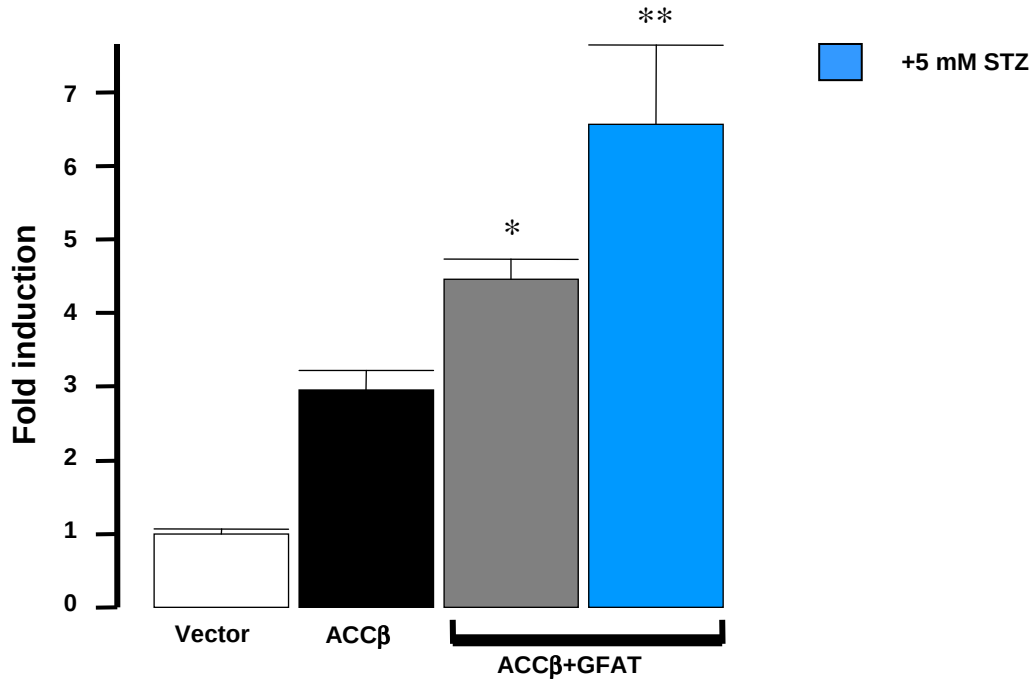

Figure 22: Pharmacological inhibition of O-GlcNAcase further increases ACCβ promoter activity.
(* p<0.001 vs. ACCβ [n=35], ** p<0.001 vs. ACCβ+GFAT [n=12]. Vector: pRL-CMV, ACCβ: pPIIβ-1317/+65, GFAT: glutamine:fructose-6-phosphate amidotransferase, STZ: Streptozotocin).

These data therefore show that the human ACCβ gene promoter is regulated by these two downstream HBP regulators, i.e. OGT and O-GlcNAcase. To further strengthen these findings I next performed experiments using both an inhibitor of GFAT (i.e. DON) and an inhibitor of O-GlcNAcase (i.e. STZ) (Figure 17). In agreement with our earlier findings, DON attenuated STZ-mediated upregulation of ACCβ promoter activity (Figure 23).

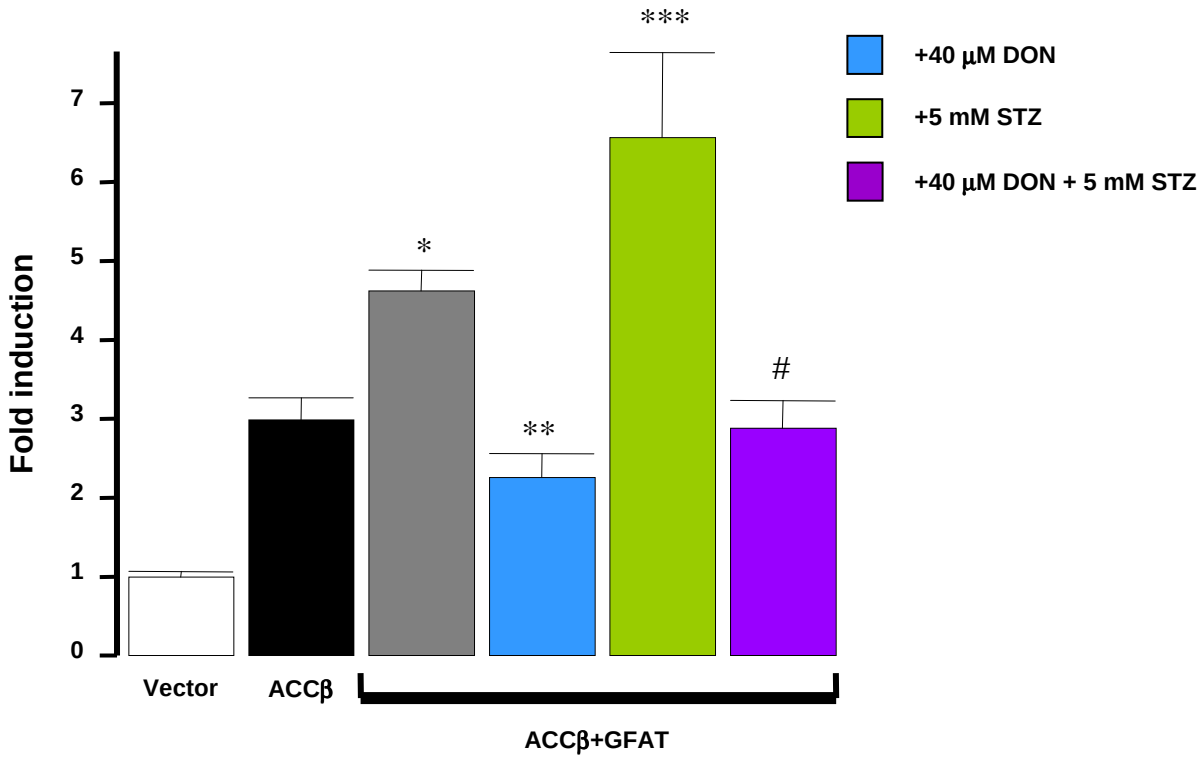

Figure 23: Pharmacological inhibition of inhibition of GFAT together with inhibition of O-GlcNAcase attenuates ACCβ promoter induction.
(∗ p<0.001 vs. ACCβ [n=33], ∗∗ p<0.001 vs. ACCβ+GFAT [n=10],∗∗∗ p<0.001 vs. ACCβ+GFAT [n=12], # p<0.05 vs. ACCβ+GFAT [n=7], # p<0.001 vs. ACCβ+GFAT+STZ [n=7]. Vector: pRL-CMV, ACCβ: pPIIβ-1317/+65, GFAT: glutamine:fructose-6-phosphate amidotransferase).

To gain further insight into transcriptional mechanisms underlying GFAT-mediated induction of ACCβ promoter activity, we employed a candidate transcription factor approach. Since our laboratory previously implicated upstream stimulatory factors (USFs) in ACCβ promoter regulation (Makaula et al., 2006) I next tested USF1 and USF2 as transcriptional regulators in the GFAT-mediated induction of ACCβ gene promoter. Here, USF2 induced ACCβ promoter activity by 44 ± 23% (p<0.001, n=6). However, when co-transfected with GFAT, USF2 did not further increase ACCβ promoter activity (Figure 24).

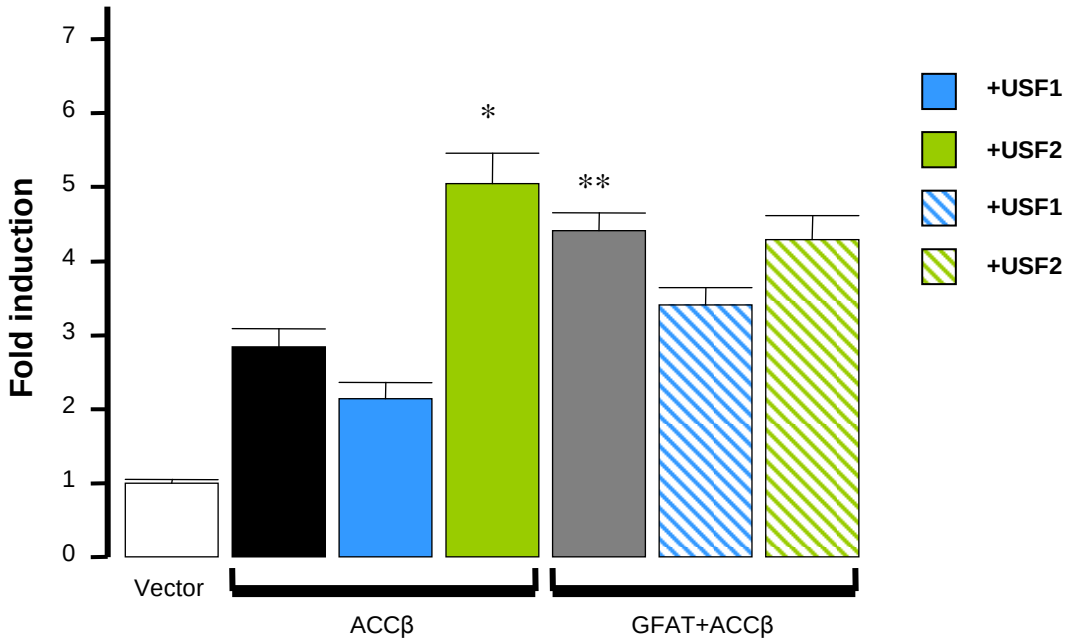

Figure 24: USF2 overexpression induces ACCβ promoter activity.
(∗ p<0.001 vs. ACCβ [n=6], ∗∗ p<0.001 vs. ACCβ [n=6]. Vector: pRL-CMV, ACCβ: pPIIβ-1317/+65, GFAT: glutamine:fructose-6-phosphate amidotransferase, USF1: upstream stimulatory factor 1, USF2: upstream stimulatory factor 2.

We further tested USF-mediated regulation of the ACCβ promoter by co-transfecting a GFAT expression construct together with a USF luciferase reporter construct (USF-L = Upstream Stimulatory Factor TransLucent™ Reporter Vector) that contains multiple promoter binding sites for USFs. Here, we found a marked induction of the USF-L reporter construct by 80 ± 12% (p<0.001, n=5) compared to the vector (Figure 25).

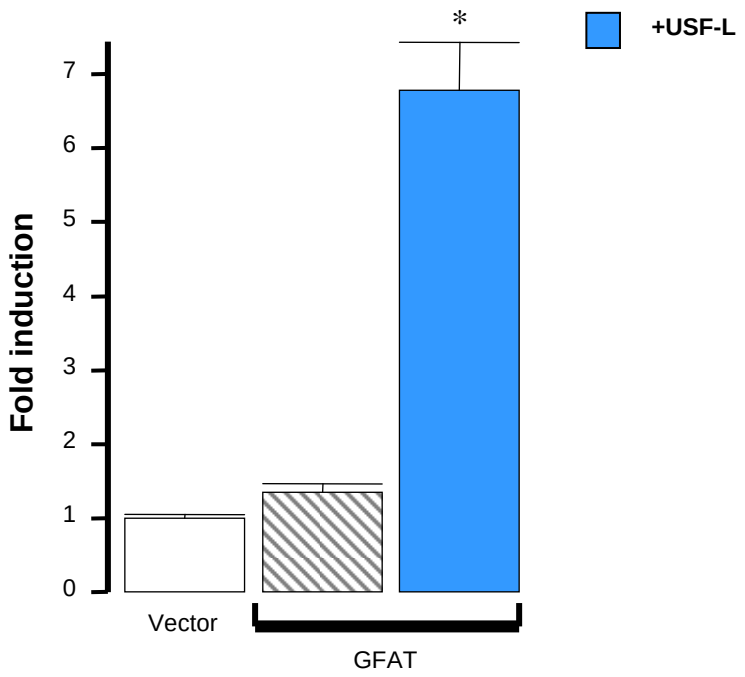

Figure 25: GFAT overexpression enhances USF transcriptional activation.
(∗ p<0.001 vs. GFAT [n=5]. Vector: pRL-CMV, ACCβ: pPIIβ-1317/+65, GFAT: glutamine:fructose-6-phosphate amidotransferase, USF-L: upstream stimulatory factor TransLucent™ Reporter Vector).

3.2. Western blotting

3.2.1. *In vitro* experiments

To assess the degree of O-GlcNAcation after transfection, we performed Western blotting using our well-established protocol. We employed an Allprep RNA/Protein extraction Kit (Qiagen, Invitrogen, Carlsbad, CA, USA) to simultaneously isolate and purify RNA and protein. Protein extracts were probed using an O-GlcNAc Western blot Detection Kit (Pierce, catalogue number 24565, Rockford, Illinois). The membrane was stripped and reprobed with β-actin antibody. Our preliminary results suggest little difference in the level of O-GlcNAc modified proteins when transfected with ACCβ ± GFAT (n=3). However, there is a decreasing trend when cells were treated with 40 µM DON (Figure 26). Additional samples need to be tested to further assess this.

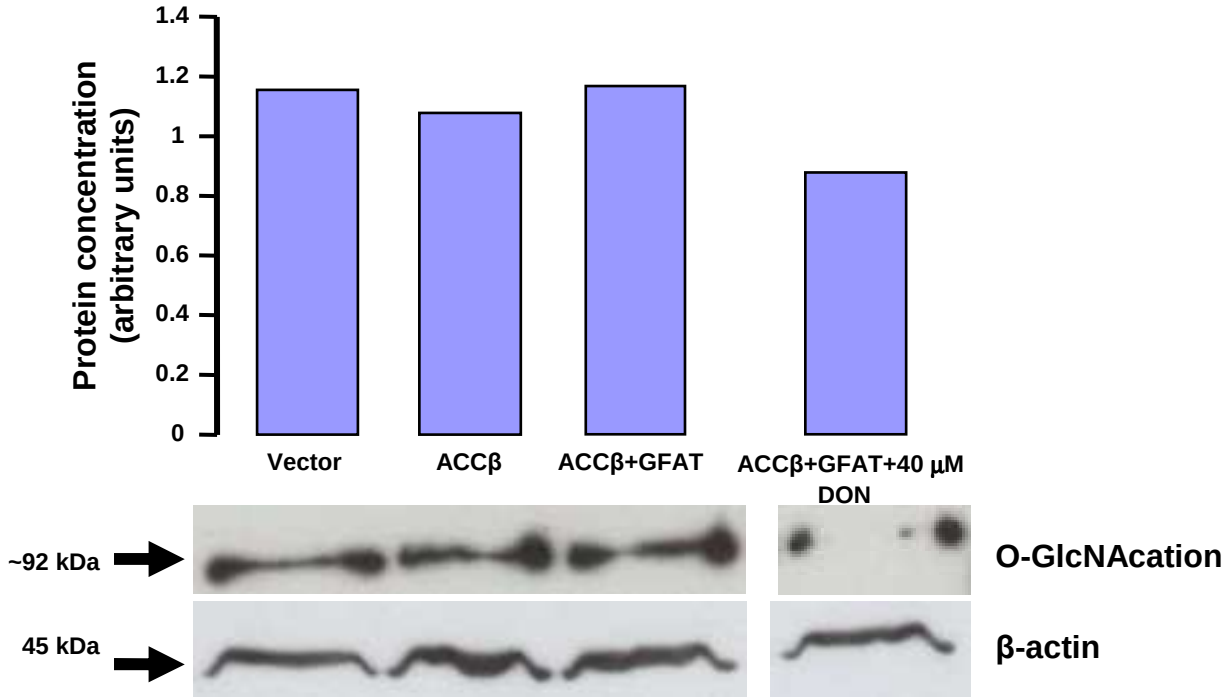

Figure 26: Degree of O-GlcNAcation after GFAT transfection into H9c2.
(The densitometry readings were normalised for protein loading using β-actin. Vector: pRL-CMV [n=1], ACCβ: pPIIβ-1317/+65 [n=3], GFAT: glutamine:fructose-6-phosphate amidotransferase [n=3], DON: 6-Diazo-5-oxo-L-norleucine [n=3]).

3.2.2. *In vivo* experiments

We investigated our hypothesis in a mouse model of type 2 diabetes. Total protein was purified from previously collected heart tissue from heterozygous (db/+) and homozygous (db/db) female mice and probed for degree of O-GlcNAcation. Due to animal limitations, we could only test 3 female db/db and 3 matched db/+ controls. Our preliminary blotting data suggest that O-GlcNAc modification of proteins are decreased in the female db/db mouse (Figure 27).

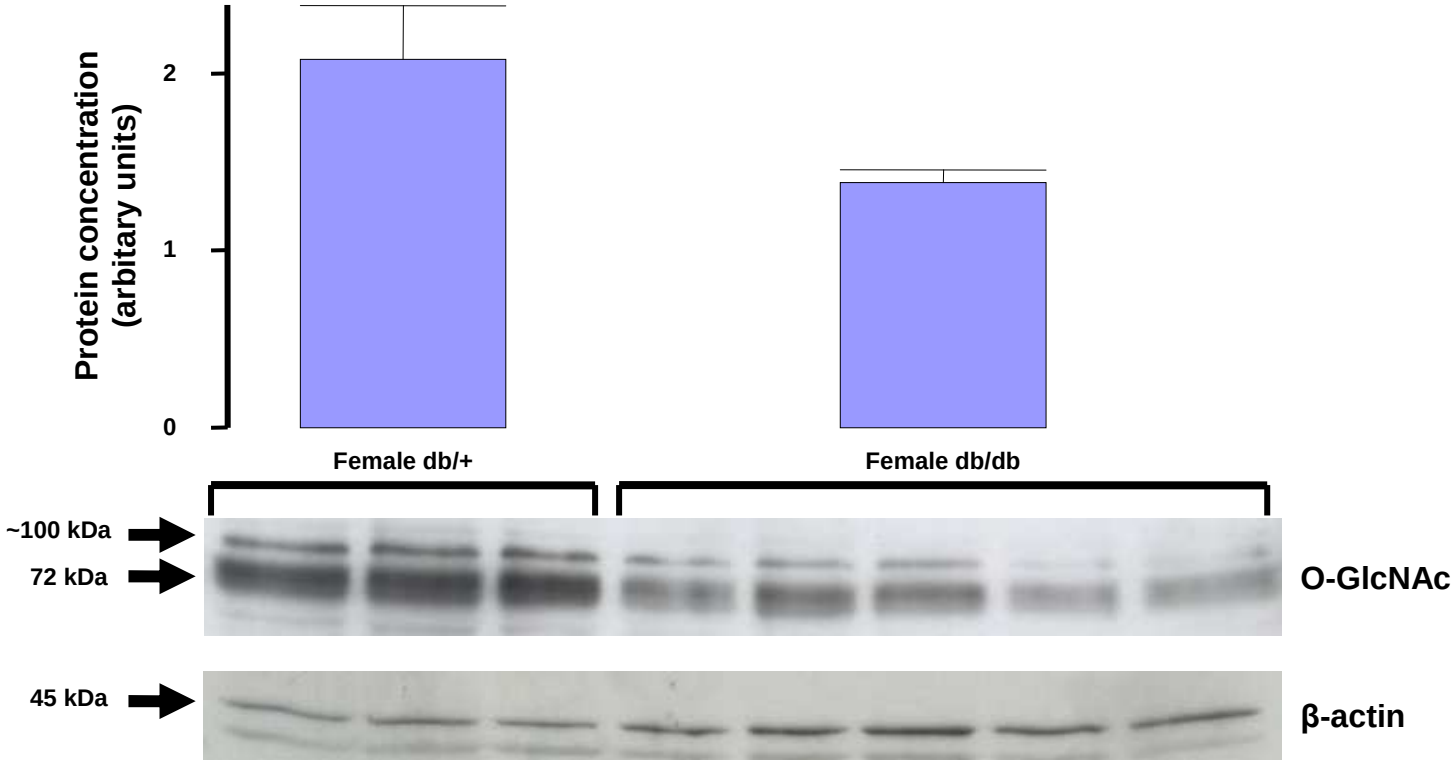

Figure 27: Degree of O-GlcNAcation in db/db female mouse heart.
(The densitometry readings were normalised for protein load using β-actin. ∗ p<0.0008 vs. female db/+ [n=3]).

To test whether alterations in O-GlcNAc modification are due to a change in GFAT expression, we also assessed GFAT peptide levels in db/db versus db/+ female mouse hearts. Our preliminary results suggest a decreasing trend in GFAT protein expression (Figure 28). However, additional sample numbers are required to confirm whether these trends are indeed true.

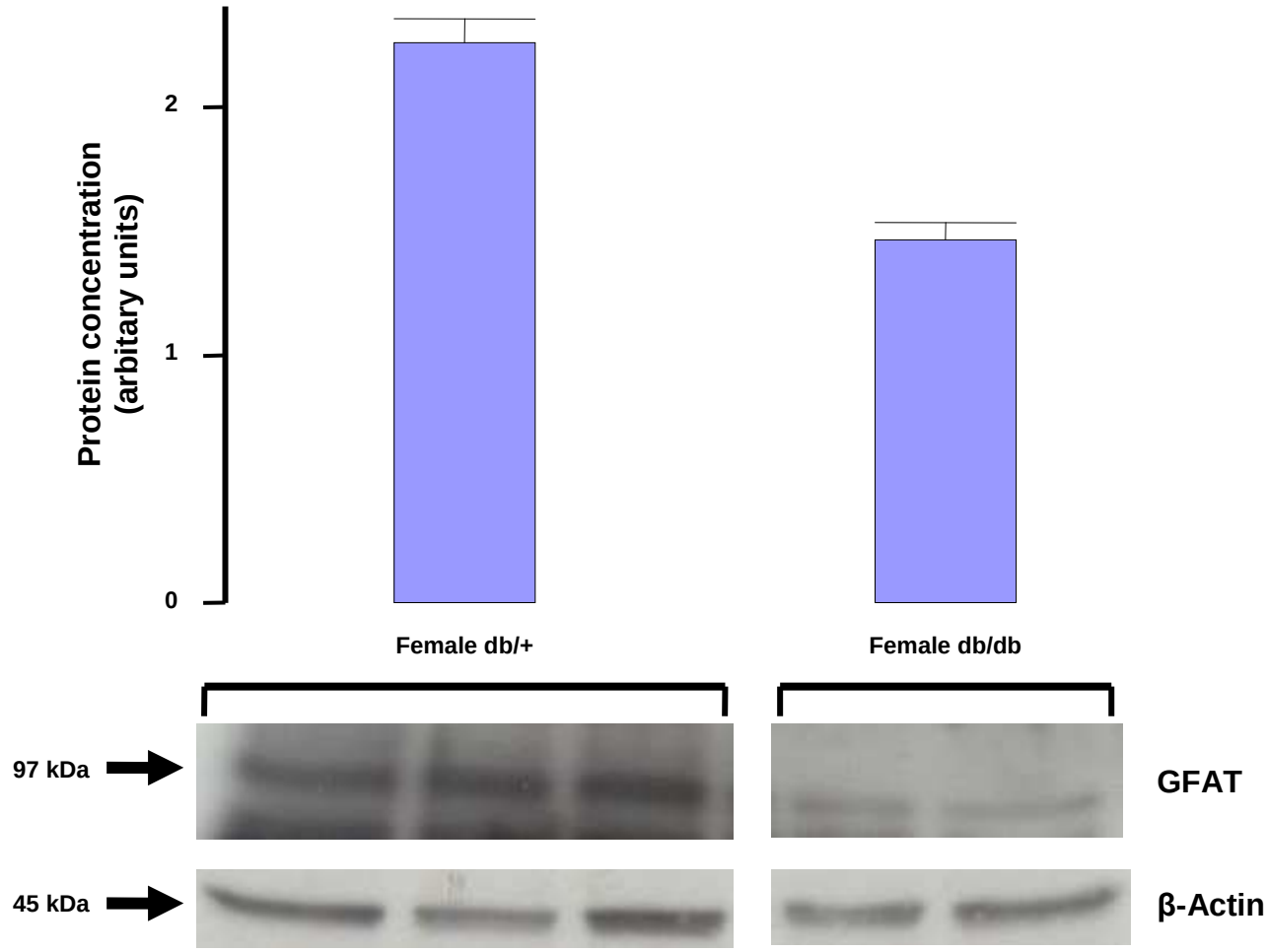

Figure 28: GFAT peptide levels in female diabetic mouse hearts.
(The densitometry readings were normalised for protein load using β-actin).

To elucidate whether these observations were gender dependent, we also analysed male db/+ and db/db mouse heart tissue using the GFAT antibody (due to time constraints we could not perform O-GlcNAc analysis for male heart tissues). Again, we were limited by sample numbers (n=3 for male db/db and db/+). Our early results suggest no differences in GFAT expression between male db/+ and db/db mice (Figure 29). However, further studies are needed to confirm our preliminary data and whether gender-dependent differences do indeed exist.

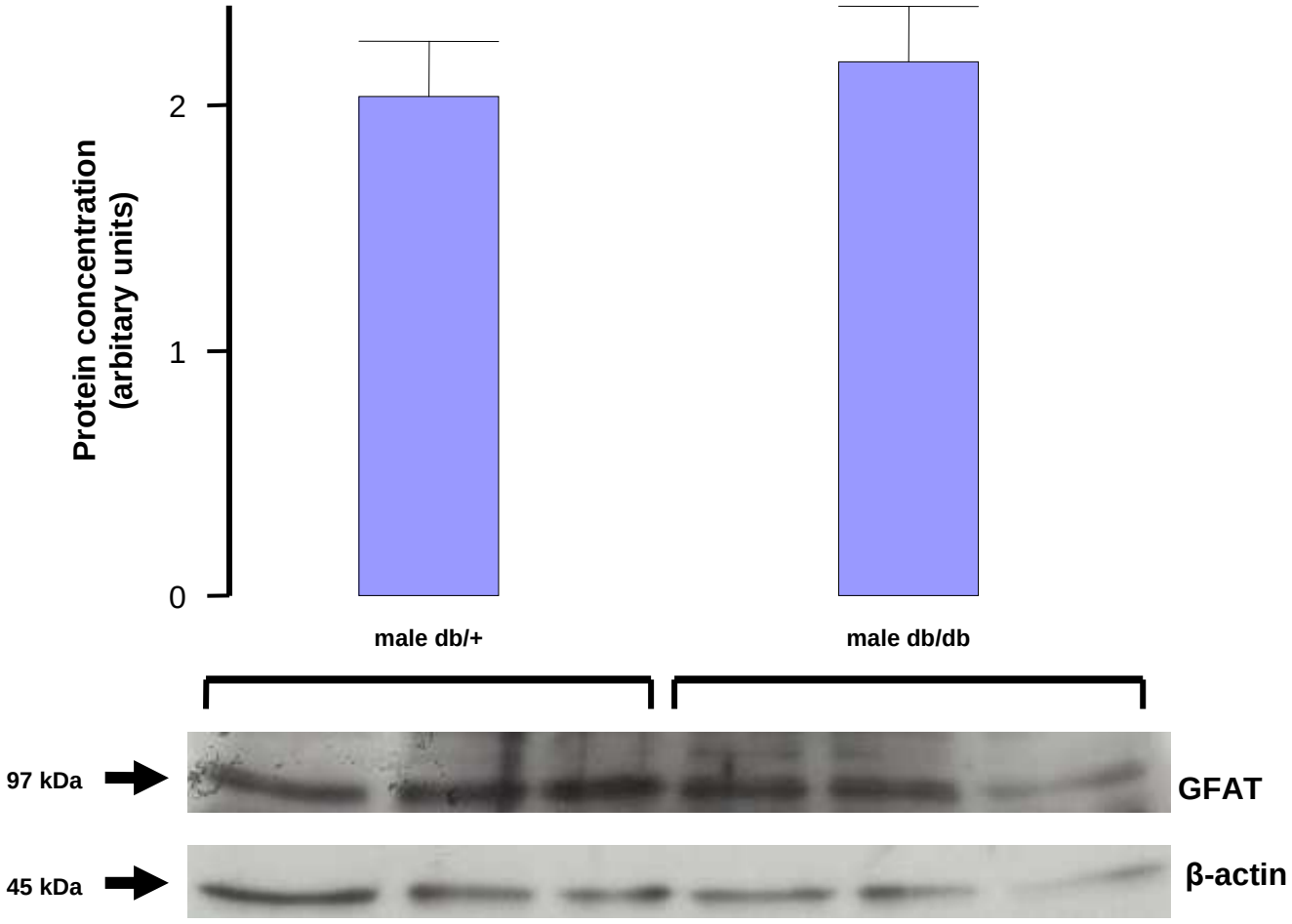

Figure 29: GFAT peptide levels in male diabetic mouse hearts.
(The densitometry readings were normalised for protein load using β-actin [n=3]).

Chapter 4

Discussion

Discussion

For this study we tested the hypothesis that increased flux through the hexosamine biosynthetic pathway (HBP) induces cardiac ACCβ gene expression. A secondary hypothesis resulting from this is that HBP-mediated induction would reduce mitochondrial fatty acid uptake/oxidation and result in an accumulation of intracellular lipid in the insulin resistant setting (hyperlipidaemia). This lipid accumulation will trigger signaling pathways resulting in cell death, insulin resistance and contractile dysfunction. The secondary hypothesis now forms part of my ongoing studies. The major novel finding of this study is that the human ACCβ gene promoter is inducible by increased flux via the HBP. Moreover we find that upstream stimulatory factors play a crucial role in transcriptional regulation of this process.

Increased flux through the hexosamine biosynthetic pathway has been linked to an increase in glucose and glucosamine availability. An increase in HBP flux results in higher UDP-GlcNAc production and a general increase in O-GlcNAc modification of a large number of proteins and transcription factors. O-GlcNAc has been shown to operate in opposition to phosphorylation, glycosylating proteins that are dephosphorylated and *vice versa* (21, 59, 65). Studies have proposed that the hexosamine biosynthetic pathway functions as a cellular nutrient sensor and numerous papers have showed a correlation between increased flux through the HBP and insulin resistance (10-12, 41, 79, 96). For example, Marshall et al. (1991) first proposed a role for glucose flux via the HBP in insulin resistance from a series of experiments performed in isolated rat adipocytes (77). Other studies found a correlation between the

HBP and insulin resistance in rodents treated with glucose/glucosamine (18, 22, 25, 51). Recently, increased O-GlcNAc modification has been attributed to altered glucose uptake resulting in insulin resistance (79, 80, 96, 132). A study investigating overexpression of OGT in adipose and muscle of mice resulting in increased O-GlcNAcation showed insulin resistance and hyperleptinaemia (81, 132). These studies would suggest that increased HBP flux and increased O-GlcNAcation can impact on fatty acid and glucose pathways. In this study we tried to confirm this *in vivo* by investigating GFAT expression and O-GlcNAc modification in the mouse heart. Although, we were able to see some differences in our results, the sample size was too small to draw any meaningful conclusions.

Several experiments completed for this study supports our primary hypothesis.

1. We found that GFAT overexpression increased ACCβ promoter activity by ~75% in cardiac myoblasts. This would suggest that increased HBP flux results in O-GlcNAc modification of transcriptional targets thereby inducing ACCβ promoter activity.

2. ACCβ gene promoter activity was induced in a dose-responsive manner to increasing glutamine concentrations (glutamine being an HBP substrate).

It is important to note that the media used in culturing cells utilises 4 mM L-glutamine for standard growing conditions. Cells that were cultured at 0 mM L-

glutamine grew slower than those at 4 mM and 8 mM L-glutamine. We therefore had to ensure that the L-glutamine concentration of our growing media maintained the same concentration for all experiments to ensure that results were reproducible. We are considering using varying doses of glucosamine (another substrate for the HBP) in future experiments.

3. Cotransfection of myoblasts with two dominant negative constructs (competitive inhibitors of GFAT) attenuated dGFAT-mediated ACCβ promoter induction.

4. Two specific pharmaceutical inhibitors of GFAT, i.e. azaserine and 6-Diazo-5-oxo-L-norleucine attenuated GFAT-induced upregulation of ACCβ.

5. To determine whether downsteam regulators were induced in this process we employed appropriate pharmaceutical inhibitors of the HBP.

The first downstream target of the HBP we chose to investigate was OGT, an enzyme that converts UDP-GlcNAc to O-GlcNAc and then binds it to serine and threonine residues of proteins, lipids and transcription factors (12, 64, 71). Alloxan (OGT inhibitor) administration reduced GFAT-induced ACCβ promoter activity. Of note, O-GlcNAcation is a very important regulatory step in developmental processes (42). Previous studies found that complete inhibition of OGT is lethal (42, 43, 86, 104). However for these experiments performed no obvious signs of large scale cell death were observed on examination under the light microscope at 10, 000 X magnification. I propose that this could be because the concentration we used was low (0.1 mM - 2 mM) and

probably did not completely inhibit OGT activity. Another possibility may be that we were investigating the HBP in rat cardiac-derived myoblasts, and hence the aforementioned concern would only be applicable to tissue and whole organ development.

We also tested a pharmaceutical inhibitor of O-GlcNAcase, i.e. streptozotocin (132). Here we found that streptozotocin treatment enhanced ACCβ promoter activity. Of note, streptozotocin is an inhibitor that is widely used to investigate type 1 diabetes (95), known to destroy pancreatic β-cells (93). However, in our model we did not observe any cell death. This was confirmed by visually comparing cell viability between wells that contained seeded cells treated ± streptozotocin between media changes on day 3 and day 4 of the transfection procedure (Figure 2 of Methods section). I propose that this is probably due to the cell type (H9c2 myoblasts) used in this study. It has also been shown that an increase in O-GlcNAcation is linked to insulin resistance (5, 14, 42, 81, 90, 120). This would explain why streptozotocin is lethal to pancreatic β-cells and why it is so effective in creating a type 1 diabetic model, i.e. the type 1 diabetes is created by destroying the insulin-producing cells after they fail to maintain β-cell compensation (16, 93). Cardiomyocytes and H9c2 myoblasts (precursor cells to cardiomyocytes) do not produce insulin or function as β-cells and thus would not be affected in this way.

To further strengthen our hypothesis we combined DON and streptozotocin since these inhibitors have opposite effects on the HBP. We found that DON decreased ACCβ promoter activity while streptozotocin increased it. Since

DON acts higher up in the HBP pathway DON inhibition probably outweighed streptozotocin inhibition, resulting in a decreased ACCβ promoter activity.

The data from transfection experiments strongly supported the hypothesis that increased flux via the HBP induces ACCβ promoter activity. However, increased HBP flux effects are expected to be mediated via O-GlcNAcated transcriptional regulation. It is likely that a number/cluster of transcription factors form a complex with each other to regulate the ACCβ promoter in response to high HBP flux. In light of this we followed a candidate transcription factor approach. Here we focused on upstream stimulatory factors since it was previously shown to upregulate the ACCβ gene promoter (75). Promoter studies in cardiomyocytes have suggested that USF1 can mediate ACCβ promoter activity in a glucose-dependent manner, but implicates the pentose phosphate pathway (75). USF1 has also been shown to induce TGF-β, which has been shown to be upregulated by the HBP (124).

These experiments were performed toward the end of my thesis and thus the results are of a preliminary nature. However, my data revealed that USF2, and not USF1, regulates ACCβ promoter activity via the HBP. When the ACCβ promoter was cotransfected with GFAT together with USF2, this did not show a further increase versus USF2 alone. This could be because a “ceiling level” of overexpression of the USF2 construct was reached.

We also cotransfected GFAT with a USF reporter-promoter construct (USF-L) containing consensus binding sites for USFs. Interestingly, the USF-L construct was induced to a much greater extent then with USF2 alone. These data therefore suggest that USF1-USF2 heterodimers may induce ACCβ to a

greater extent. In agreement, other studies have shown that USF1 and USF2 can form either homo- or heterodimers (107, 119).

USF1 has also been associated with the metabolic syndrome and type 2-diabetes (83). Due to time constraints I could not perform a conventional transfection with USF1 and USF2 together. Unfortunately, due to a limitation of animal numbers and time constraints our Western blotting results can only be considered as preliminary. Preliminary results of Western blotting showed that O-GlcNAcation was increased when the cells were cotransfected with GFAT and ACCβ reporter-promoter construct but that O-GlcNAcation decreased when the myoblasts were treated with DON. In our preliminary mouse studies we saw a reduction of GFAT protein in the female db/db from control (db/+) but saw no significant difference in the male mice. We also found a decrease in O-GlcNAcation of proteins in female db/db from control (db/+). Further experiments will have to be carried out before any assumptions can be made as to the relevance of this data. Although, we can speculate that an inability of the male diabetic heart to reduce CPT1 inhibition could explain why female hearts show a relatively higher degree of protection compared to male hearts (30, 56, 116). Should this be found to be the case, we may assume that hormones such as estrogen or testosterone may be involved in the regulation of the HBP.

Conclusion

Our data reveal a novel finding, i.e. that increased flux through the hexosamine biosynthetic pathway activates USFs thereby inducing ACCβ gene promoter activity in cardiac-derived myoblasts (Figure 30). To date no data, as far as I am aware, has been published in this regard. Further studies are underway to test our secondary hypothesis, i.e. that HBP-induced ACCβ induction reduces fatty acid oxidation, thereby leading to intracellular lipid accumulation due to a mismatch between sarcolemmal FA uptake and mitochondrial FA oxidation in the insulin resistant setting (Figure 30). Subsequently, we propose that intramyocardial lipid accumulation triggers signaling pathways resulting in cell death, insulin resistance and contractile dysfunction.

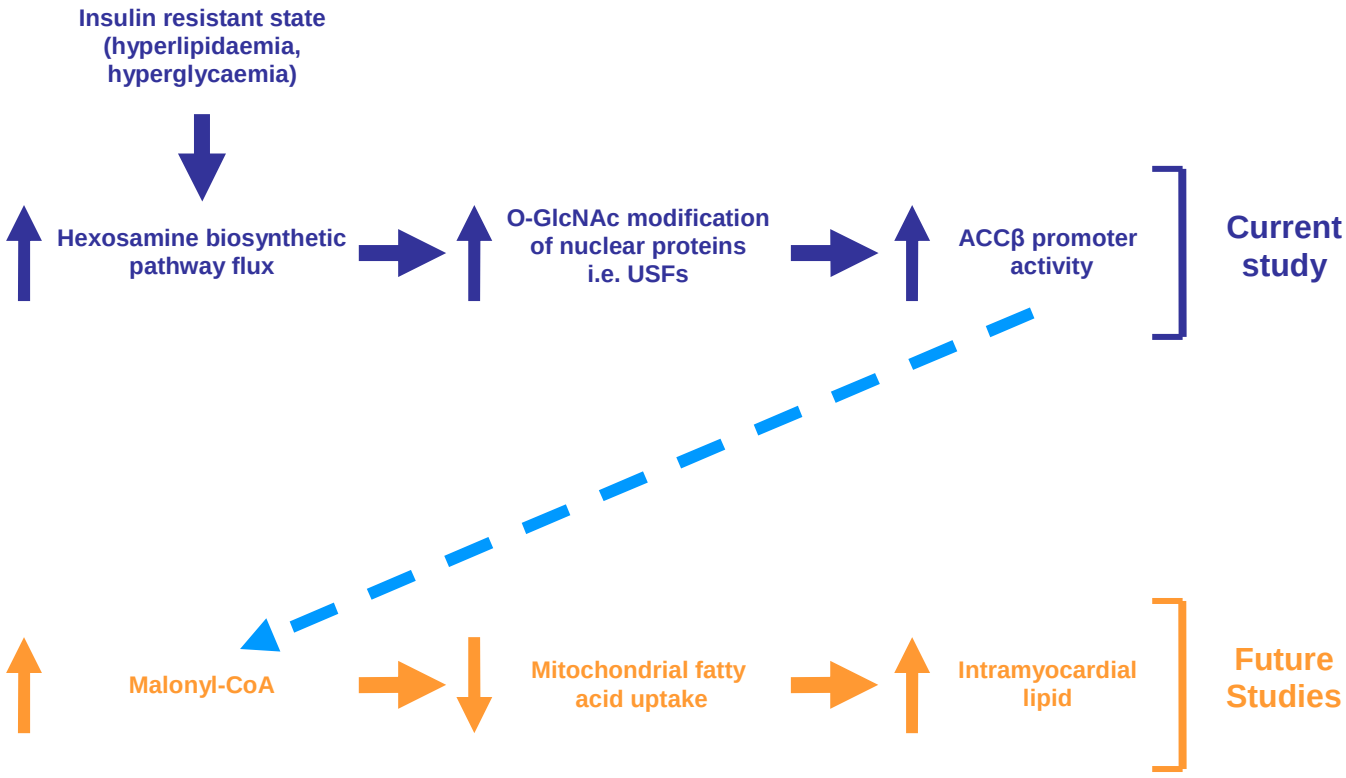

Figure 30: Schematic diagram of completed studies and planned future investigations.

Limitations

A limitation of the transfection technique is the time it takes to optimise the transfection protocol. This limited the initial progress of this project.

The effectiveness of an inhibitor of any pathway is determined by its specificity for its target. The inhibitors we employed for our experiments are well documented in the literature (17, 132). We tried to use as many inhibitors for the same target site as we could to strengthen our results. However, we are aware these inhibitors could also inhibit/enhance other intracellular signaling pathways. However, we also employed two dominant negative GFAT constructs which considerably strengthened our data.

Due to time constraints and limitation on animal numbers we were unable to investigate the differences in regulation of the HBP between male and female db/db mice. This means that our Western blotting results are only preliminary and more experiments would have to be performed to confirm this result.

Future Studies

- We are currently performing real-time PCR on RNA extracted from transfected myoblasts to determine whether the increase in ACCβ promoter activity results in a concomitant increase in endogenous RNA expression.

- We will also be performing additional USF transfection experiments and DNA binding assays (ELISAs and CHiP) to confirm the role of USF1 and USF2 in the transcriptional regulation of ACCβ.

- We would also like to confirm our L-glutamine transfection experiments by administering different doses of glucosamine to transfected myoblasts. Since it is more potent than L-glutamine, we expect to see a greater effect on ACCβ promoter activity.

- We are also currently investigating an additional inhibitor, i.e. O-(2-acetamido-2-deoxy-D-glucopyranosylidene) amino-*N*-phenylcarbamate (PUGNAc) (132), proposed to be more potent than streptozotocin.

- We also intend to probe heart tissues from various type-2 diabetic rodent models (db/db, Zucker and diet-induced rat model).

- To investigate our secondary hypothesis we will measure fatty acid accumulation with oil red staining and measure malonyl-CoA levels (Figure 30).

References

1. **Abu-Elheiga L, Almarza-Ortega DB., Baldini A., and Wakil SJ.** Human acetyl-CoA carboxylase 2. Molecular cloning, characterization, chromosmal mapping, and evidence for two isofroms. *J Biol Chem*272: 10669-10677, 1997.

2. **Abu-Elheiga L, Brinkley WR., Zhong L., Chirala SS., Woldegiorgis G., and Wakil SJ.** The subcellular localization of acetyl-CoA carboxylase2. *Proc Natl Acad Sci U S A*97: 1444-1449, 2000.

3. **Abu-Elheiga L, Jayakumar A., Baldini A., Chirala SS., and Wakil SJ.** Human acetyl-CoA carboxylase: characterization, molecular cloning, and evidence for two isoforms. *Proc Natl Acad Sci U S A*92: 4011-4015, 1995.

4. **Ali A, and Crowther NJ.** Body fat distribution and insulin resistance. *S Afr Med J*95: 878-880, 2005.

5. **Arias E, Kim J., and Cartee, GD.** Prolonged incubation in PUGNAc results in increased protein O-linked glycosylation and insulin resistance in rat skeletal muscle. *Diabetes*53: 921-930, 2004.

6. **Baron A, Zhu JS., Weldon J., Maianu L., and Garvey WT.** Glucosamine induces insulin resistance in vivo by affecting GLUT 4 translocation in skeletal muscle-Implications for glucose toxicity. *J Clin Invest*96: 2792-2801, 1995.

7. **Bian F, Kasumov T., Jobbins KA., Minkler PE., Anderson VE., Kerner J., Hoppel CL., and Brunengraber H.** Competition between acetate and oleate for the formation of malonyl-CoA and mitochondrial acetyl-CoA in the perfused rat heart. *J Mol Cell Cardiol*41: 868-875, 2006.

8. **Brinkmann J, Abumrad NA., Ibrahimi A., van der Vusse GJ., and Glatz JF.** New insights into long-chain fatty acid uptake by heart muscle: a crucial role for fatty acid translocase/CD36. *Biochem J*367: 561-570, 2002.

9. **Brooks G.** Intra- and extra-cellular lactate shuttles. *Med Sci Sports Exerc*32: 790-799, 2000.

10. **Brownlee M.** Biochemistry and molecular cell biology of diabetic complications. *Nature*414: 813-820, 2001.

11. **Brownlee M.** The pathobiology of diabetic complications: a unifying mechanism. *Diabetes*54: 1615-1625, 2005.

12. **Buse M.** Hexosamines, insulin resistance and the complications of diabetes: current status. *Am J Physiol Endocrinol Metab*290: E1-E8, 2006.

13. **Buse M, Robinson KA., Gettys TW., McMahon EG., and Gluve EA.** Increased activity of the hexosamine synthesis pathway in muscles of insulin-resistant ob/ob mice. *Am J Physiol Endocrinol Metab*272: E1080-E1088, 1997.

14. **Buse M, Robinson KA., Marshall BA., Hresko RC., and Mueckler MM.** Enhanced O-GlcNAc protein modification is associated with insulin resistance in GLUT1- overexpressing muscles. *Am J Physiol Endocrinol Metab*283: E241-E250, 2002.

15. **Carley A, and Severson, DL.** Fatty acid metabolism is enhanced in type 2 diabetic hearts. *Biochim Biophys Acta*1734: 112-126, 2005.

16. **Cavaghan M, Ehrmann DA., and Polonsky KS.** Interactions between insulin resistance and insulin secretion in the development of glucose intolerance. *J Clin Invest*106: 329-333, 2000.

17. **Champattanachai V, Marchase RB., and Chatham J.** Glucosamine protects neonatal cardiomyocytes from ischemia-reperfusion injury via

increases protein-associated O-GlcNAc. *Am J Physiol Cell Physiol* 292: C178-C187, 2006.

18. **Chen H, Ing BL., Robinson KA., Feagin AC., Buse MG., and Quon MJ.** Effects of overexpression of glutamine:fructose-6-phosphate amidotransferase (GFAT) and glucosamine treatment on translocation of GLUT 4 in rat adipose cells. *Mol Cell Endocrinol* 1997: 67-77, 1997.

19. **Chien K.** Alchemy and the New Age of Cardiac Muscle Cell Biology. *PLoS Biol* 3: e131, 2005.

20. **Cipollo J, Antoine Awad A., Costello CE., Robbins PW., and Hirschberg CB.** Biosynthesis in vitro of Caenorhabditis elegans phosphorylcholine oligosaccharides. *Proc Natl Acad Sci USA* 101: 3404-3408, 2004.

21. **Comer F, and Hart GW.** O-GlcNAc and the control of gene expression. *Biochim Biophys Acta* 1473: 161-171, 1999.

22. **Cooksey R, Hebert LF Jr., Zhu JH., Wofford P., Garvey WT., and McClain DA.** Mechanism of hexosamine-induced insulin resistance in transgenic mice overexpressing glutamine:fructose-6-phosphate

amidotransferase: decreased glucose transporter GLUT 4 translocation and reversal by treatment with thiazolidinedione. *Endocrinology*140: 1151-1157, 1999.

23. **Coort S, Bonen A., van der Vusse GJ., Glatz JFF., and Luiken JJFP.** Cardiac substrate uptake and metabolism in obesity and type-2 diabetes: Role of sarcolemmal substrate transporters. *Mol Cell Biol*299: 5-18, 2007.

24. **Corden J.** Tails of RNA polymerase II. *Trends Biochem Sci*15: 383-387, 1990.

25. **Crook E, Daniels MC., Smith TM., and McClain DA.** Regulation of insulin-stimulated glycogen synthase activity by overexpression of glutamine:fructose-6-phosphate amidotransferase in rat-1 fibroblasts. *Diabetes*42: 1289-1296, 1993.

26. **Dahmus M.** Phosphorylation of the C-terminal domain of RNA polymerase II. *Biochim Biophys Acta*1261: 171-182, 1995.

27. **Dyck J, and Lopaschuk GD.** AMPK alterations in cardiac physiology and pathology: enemy or ally? *J Physiol*574: 95-112, 2006.

28. **Dyck J, Cheng JF., Stanley WC., Barr R., Chandler MP., Brown S., Wallace D., Arrhenius T., Harmon C., Yang G., Nadzan AM., and Lopaschuk GD.** Malonyl coenzyme a decarboxylase inhibition protects the ischemic heart by inhibiting fatty acid oxidation and stimulating glucose oxidation. *Circ Res* 94: e78-e84, 2004.

29. **Eaton S.** Control of mitochondrial beta-oxidation flux. *Prog Lipid Res* 41: 197-239, 2002.

30. **Essop M, Chan WY., and Taegtmeyer H.** Metabolic gene switching in the murine female heart parallels enhanced mitochondrial respiratory function in response to oxidative stress. *FEBS J*274: 5278-5284, 2007.

31. **Federici M, Menghini R., Mauriello A., Hribalm ML., Ferelli F., Lauro D., Sbraccia P., Spagnoli LG., Sesti G., and Lauro R.** Insulin-dependent activation of endothelial nitric oxide synthetase is impaired by O-linked glycosylation of signaling proteins in human coronary endothelial cells. *Circ* 106: 466-472, 2002.

32. **Freiberg C, Pohlmann J., Nell PG., Endermann R., Schuhmacher J., Newton B., Otteneder M., Lampe T., Häbich D., and Ziegelbauer K.** Novel

Bacterial Acetyl Coenzyme A Carboxylase Inhibitors with Antibiotic Efficacy In Vivo. *Antimicrob Agents Chemother*50: 2707-2712, 2006.

33. **Garland P, and Randle PJ.** Control of pyruvate dehydrogenase in the perfused rat heart by the intracellular concentration of acetyl-coenzyme A. *Biochem J*91: 6c, 1964.

34. **Ghisla S.** Beta-oxidation of fatty acids. A century of discovery. *Eur J Biochem*271: 459-461, 2004.

35. **Gilde A, and Van Bilsen M.,.** Peroxisome proliferator-activated receptors (PPARs): regulators of gene expression in heart and skeletal muscle. *Acta Physiol Scand*178: 425-434, 2003.

36. **Giordano F.** Oxygen, oxidative stress, hypoxia, and heart failure. *J Clin Invest*115: 500-508, 2005.

37. **Gladden L.** Lactate metabolism: a new paradigm for the third millenium. *J Physiol*558: 5-30, 2004.

38. **Grepin C, Dagnino L., Robitaille L., Haberstroh L., Antakly T., and Nemer M.** A Hormone-Encoding Gene Identifies a Pathway for Cardiac but Not Skeletal Muscle Gene Transcription. *Mol Cell Biol*14: 3115-3129, 1994.

39. **Ha J, Lee JK., Kim KS., Witters LA., and Kim KH.** Cloning of human acetyl-CoA carboxylase-beta and its unique features. *Proc Natl Acad Sci USA* 93: 11466-11470, 1996.

40. **Hamilton J, and Kamp F.** How are free fatty acids transported in membranes? Is it by proteins or by free diffusion through the lipids? *Diabetes* 48: 2255-2269, 1999.

41. **Hammes H, Du X., Edelstein D., Taguchi T., Matsumura T., Ju Q., Lin J., Bierhaus A., Nawroth P., Hannak D., Neumaier M., Bergfeld R., Giardino I., and Brownlee M.** Benfotiamine blocks three major pathways of hyperglycemic damage and prevents experimental diabetic retinopathy. *Nat Med*9: 294-299, 2003.

42. **Hanover J, Forsythe ME., Henessey PT., Brodigan TM., Love DC., Ashwell G., and Krause M.** A Caenorhabditis elegans model of insulin resistance: Altered macronutrient storage and dauer formation in an OGT-1 knockout. *Proc Natl Acad Sci USA*102: 11266-11271, 2005.

43. **Hanover J, Yu S., Lubas WB., Shin SH., Ragano-Caracciola M., Kochran J., and Love DC.,.** Mitochondrial and nucleocytoplasmic isoforms of

O-linked GlcNAc transferase encoded by a single mammalian gene. *Arch Biochem Biophys* 409: 287-297, 2003.

44. **Harada N, Oda Z., Hara Y., Fujinami K., Okawa M., Ohbuchi K., Yonemoto M., Ikeda Y., Ohwaki K., Aragane K., Tamai Y., and Kusunoki J.** Hepatic De Novo Lipogenesis Is Present IN Liver-Specific ACC1-deficient Mice. *Mol Cell Biol* 27: 1881-1888, 2007.

45. **Hart G.** Glycosylation. *Curr Opin Cell Biol* 4: 1-17-1023, 1992.

46. **Hasselbaink D, Glatz JFC., Luiken JJFP., Roemen THM., and van der Vusse GJ.** Ketone bodies disturb fatty acid handling in isolated cardiomyocytes derived from control and diabetic rats. *Biochem J* 371: 753-760, 2003.

47. **Hawkins M, Angelov I., Lui R., Barzilai N., and Rosetti L.** The tissue concentration of UDP-*N*acetylglucosamine modulates the stimulatory effect of insulin on skeletal muscle glucose uptake. *J Biol Chem* 272: 4889-4895, 1997.

48. **Hawkins M, Barzilai N., Lui R., Hu M., Chen W., and Rosetti L.** Role of the glucosamine pathway in fat-induced insulin resistance. *J Clin Invest*99: 2173-2182, 1997.

49. **Hawkins. M, Barzilai N., Chen W., Angelov I., Hu M., Cohen P., and Rosetti L.** Increased hexosamine availability similarly impairs the action of insulin and IGF-1 on glucose disposal. *Diabetes*45: 1734-1743, 1996.

50. **Heart E, Choi WS., and Sung CK.** Glucosamine-induced insulin resistance in 3T3-L1 adipocytes. *Am J Physiol Endocrinol Metab*278: E103-E112, 2000.

51. **Hebert L, Daniels MC., Zhou JX., Crook ED., Turner RL., Simmons ST., Neidigh JL., Zhu JS., Baron AD., and McClain DA.** Overexpression of glutamine:fructose-6-phosphate amidotransferase in transgenic mice leads to insulin resistance. *J Clin Invest*98: 930-936, 1996.

52. **Heese-Peck A, Cole RN., Borkhsenious ON., Hart GW., and Raikhel NV.** Plant nuclear pore complex proteins are modified by novel oligosaccharides with terminal *N*acetylglucosamine. *Plant Cell*7: 1459-1471, 1995.

53. **Herman M, and Khan BM.** Glucose transport and sensing in the maintenance of glucose homeostasis and metabolic harmony. *J Clin Invest* 116: 1767-1775, 2006.

54. **Hopkins T, Dyck JR., and Lopaschuk GD.** AMP-activated protein kinase regulation of fatty acid oxidation in the ischaemic heart. *Biochem Soc Trans*31: 207-212, 2003.

55. **Hresko R, Heimberg H., Chi MMY., and Mueckler M.** Glucosamine-induced insulin resistance in 3T3-L1 adipocytes is caused by depletion of intracellular ATP. *J Biol Chem*273: 20658-20668, 1998.

56. **Imahashi K, Pott C., Goldhaber JI., Steenbergen C., Philipson KD., and Murphy E.** Cardiac-Specific Ablation of the Na+-Ca2+ Exchanger Confers Protection Against Ischemia/Reperfusion Injury. *Circ Res*97: 916-921, 2005.

57. **Kabashima T, Kawaguchi T., Wadzinski BE., and Uyeda K.** Xylulose 5-phosphate mediates glucose-induced lipogenesis by xylulose 5-phosphate-activated protein phosphatase in rat liver. *Proc Natl Acad Sci USA*100: 5107-5112, 2003.

58. **Kasahara H, Usheva A., Ueyama T., Aoki H., Horikoshi N., and Izumo S.** Characterization of homo- and heterodimerization of cardiac Csx/Nkx2.5 homeoprotein. *J Biol Chem*276: 4570 4580, 2001.

59. **Kelly W, Dahmus ME., and Hart GW.** RNA ploymerase II is a glycoprotein: modification of the C-terminal domain by O-GlcNAc. *J Biol Chem* 268: 10416-10424, 1993.

60. **Kenchaiah D, Evans JC., Levy D., Wilson PWF., Benjamin EJ., Larson MG., Kannel WB., and Vasan RS.** Obesity and the risk of heart failure. *N Engl J Med*347: 305-313, 2002.

61. **Kim K.** Regulation of mammalian acetyl-coenzyme A carboxylase. *Annu Rev Nutr*17: 77-99, 1997.

62. **Kim YB ZJ, Zierath JR., Shen HQ., Baron AD., and Kahn BB.** Glucosamine infusion in rats rapidly impairs insulin stimulation of phosphoinositide 3-kinase but does not alter activation of Akt/protein kinase B in skeletal muscle. *Diabetes*48: 310-320, 1999.

63. **Komuro I, and Izumo S.** Csx: a murine homeobox-containing gene specifically expressed in the developing heart. *Proc Natl Acad Sci USA* 90: 8145 - 8149, 1993.

64. **Kreppel L, Blomberg MA., and Hart GW.** Dynamic glycosylation of nuclear and cytosolic proteins. Cloning and characterization of a unique O-GlcNAc transferase with multiple tetratricopeptide repeats. *J Biol Chem* 272: 9308-9315, 1997.

65. **Ku N, and Omary MB.** Expression, glycosylation, and phosphorylation of human keratins 8 18 in insect cells. *Exp Cell Res* 211: 24-35, 1994.

66. **Kudo N, Barr AJ., Barr RL., Desai S., and Lopaschuk GD.** High rates of fatty acid oxidation during reperfusion of ischemic hearts are associated with a decrease in malonyl-CoA levels due to an increase in 5'-AMP-activated protein kinase inhibition of acetyl-CoA carboxylase. *J Biol Chem* 270: 17513-17520, 1995.

67. **Lee J, Moon YA., Ha JH., Yoon DJ., Ahn YH., and Kim KS.** Cloning of human acetyl-CoA carboxylase beta promoter and its regulation by muscle regulatory factors. *J Biol Chem* 276: 2576-2585, 2001.

68. **Lopaschuk G, Folmes CDL., and Stanely WC.** Cardiac Energy Metabolism in Obesity. *Circ Res*101: 335-347, 2007.

69. **Lorenz M, and Fink GR.** Life and Death in a Macrophage: Role of the Glyoxylate Cycle in Virulence. *Eukaryot Cell*1: 657-662, 2002.

70. **Lorenzi M.** The polyol pathway as a mechanism for diabetic retinopathy: attractive, elusive, and resilient. *Exp Diabetes Res*2007: 1-10, 2007.

71. **Lubas W, Frank DW., Krause M., and Hanover JA.** *O*linked GlcNAc transferase is a conserved nucleocytoplasmic protein containing tetratricopeptide repeats. *J Biol Chem*272: 9316-9324, 1997.

72. **Luiken J, Schaap FG., van Nieuwenhoven FA., van der Vusse GJ., Bonen A., and Glatz JF.** Cellular fatty acid transport in heart and skeletal muscle is fascilitated by proteins. *Lipids*34: S169-S175, 1999.

73. **Luiken J, van Nieuwenhoven FA., America G., van der Vusse GJ., and Glatz JF.** Uptake and metabolism of palmitate by isolated cardiac myocytes from adult rats: involvement of sarcolemmal proteins. *J Lipid Res*38: 745-758, 1997.

74. **Majumdar G, Harmon A., Candelaria Martinez-Hernandez A., Raghow R., and Solomon SS.** O-glycosylation of Sp1 and transcriptional regulation of the calmodulin gene by insulin and glucagon. *Am J Physiol*285: E584-E591, 2003.

75. **Makaula S, Adam T., and Essop MF.** Upstream stimulatory factor 1 transactivates the human gene promoter of the cardiac isoform of acetyl-CoA carboxylase. *Arch Biochem Biophys*446: 91-100, 2006.

76. **Mao J, DeMayo FJ., Li H., Abu-Elheiga L., Gu Z., Shaikenov TE., Kodari P., Chirala SS., Heird WC., and Wakil SJ.** Liver-specific deletion of acetyl-CoA carboxylase 1 reduces hepatic triglyceride accumulation without affecting glucose homeostasis. *Proc Natl Acad Sci USA*103: 8552-8557, 2006.

77. **Mashall S, Bacote V., and Traxinger RR.** Discovery of a metabolic pathway mediating glucose-induced desensitization of the glucose transport system. Role of hexosamine biosynthesis in the induction of insulin resistance. *J Biol Chem*266: 4706-4712, 1991.

78. **Mashall S, Garvey WT., and Traxinger RR.** New insights into the metabolic regulation of insulin action and insulin resistance: role of glucose and amino acids. *FASEB J*5: 3031-3036, 1991.

79. **McClain D.** Hexosamines as mediators of nutrient sensing and regulation in disease. *J Diabetes Complications*16: 72-80, 2002.

80. **McClain D, Crook ED.** Hexosamines and insulin resistance. *Diabetes* 45: 1003-1009, 1996.

81. **McClain D, Lubas WA., Coosey RC., Hazel M., Parker GJ., Love DC., and Hanover JA.** Altered glycan-dependent signaling induces insulin resistance and hyperleptinemia. *Proc Natl Acad Sci USA*99: 10695-10699, 2002.

82. **Miranda P, DeFronzo RA., Califf RM., and Guyton JR.** Metabolic syndrome: definition, pathology, and mechanisms. *Am Heart J*149: 33-45, 2005.

83. **Miyake K, So WY., Poon EW., and Lam VK.** The linkage and association of the gene encoding upstream stimulatory factor 1 with type 2

diabetes and metabolic syndrome in the Chinese population. *Diabetologia* 48: 2018-2024, 2005.

84. **Molkentin JD, Lin, Q., Duncan, S. A., and Olson, E. N. 1997 ( )** Requirement of the transcription factor GATA4 for heart tube formation and ventral morphogenesis. *Genes Dev* 11: 1061 - 1072, 1997.

85. **Neely J, Denton RM., England PJ., and Randle PJ.** The Effects of Increased Heart Work on the Tricarboxylate Cycle and its Interactions with Glycolysis in the Perfused Rat Heart. *Biochem J* 128: 147-159, 1972.

86. **O'Donnell N, Zachara NE., Hart GW., and Marth JD.** OGT-dependent X-chromosome-linked protein glycosylation is a requisite modification in somatic cell function and embryo viability. *Mol Cell Biol* 24: 1680-1690, 2004.

87. **Oh S, Lee M-Y., Kim J-M., Yoon S., Shin S., Park YN., Ahn Y-H., and Kim K-S.** Alternative usages of multiple promoters of the acetyl-CoA carboxylase gene are related to differential transcriptional regulation in human and rodent tissues. *J Biol Chem* 280: 5909-5916, 2005.

88. **Olson E, and Srivastava D.** Molecular pathways controlling heart development. *Science* 272: 671 - 676, 1996.

89. **Onay-Besikci A, Campbell FM., Hopkins TA., Dyck JR., and Lopaschuk GD.** Relative importance of malonyl CoA and carnitine in maturation of fatty acid oxidation in newborn rabbit heart. *Am J Physiol Heart Circ Physiol* 284: H283-H289, 2003.

90. **Park S, Ryu J., and Lee W.** O-GlcNAc modification on IRS-1 and Akt2 by PUGNAc inhibits their phosphorylation and induces insulin resistance in rat primary adipocytes. *Exp Mol Med* 37: 220-229, 2005.

91. **Pettersson I, Muccioli G., Granata R., Deghenghi R., Ghigo E., Ohlsson C., and Isgaard J.** Natural (ghrelin) and synthetic (hexarelin) GH secretagogues stimulate H9c2 cardiomyocyte cell proliferation. *J Endocrinol* 175: 201-209, 2002.

92. **Pownall H, and Hamilton JA.** Energy translocation across cell membranes and membrane models. *Acta Physiol Scand* 178: 357-365, 2003.

93. **Prentki M, and Nolan CJ.** Islet β cell failure in type 2 diabetes. *J Clin Invest* 116: 1802-1812, 2006.

94. **Robinson K, Sens DA., and Buse MG.** Pre-exposure to glucosamine induces insulin resistance of glucose transport and glycogen synthesis in

isolated rat skeletal muscles. Study of mechanisms in muscle and rat-1 fibroblasts overexpressing the human insulin receptor. *Diabetes*42: 1333-1346, 1993.

95. **Robinson K, Weinstein ML., Lindenmayer GE., and Buse MG.** Effects of Diabetes and Hyperglycemia on the Hexosamine Synthesis Pathway in Rat Muscle and Liver. *Diabetes*44: 1438-1446, 1995.

96. **Rossetti L.** Perspective: hexosamines and nutrient sensing. *Endocrinology*141: 1922-1925, 2000.

97. **Ruderman N, Saha AK., Vavvas D., and Witters LA.** Malonyl-CoA, fuel sensing, and insulin resistance. *Am J Physiol*276: E1-E18, 1999.

98. **Rudnicki M, and Jaenisch R.** The MyoD family of transcription factors and skeletal myogenesis. *Bioessays*17: 203-209, 1995.

99. **Sabourin L, and Rudnicki MA.** The molecular regulation of myogenesis. *Clinical genetics*57: 16-25, 2000.

100. **Saddik M, Gamble J., Witters LA., and Lopaschuk GD.** Acetyl-CoA carboxylase regulation of fatty acid oxidation in the heart. *J Biol Chem*268: 25836-25845, 1993.

101. **Saha A, Schwarsin AJ., Roduit R., Masse F., Kaushik V., Tornheim K., Prentki M., and Ruderman NB.** Activation of malonyl-CoA decarboxylase in rat skeletal muscle by contraction and the AMP-activated protein kinase activator 5-aminoimidazole-4-carboxamide-1-β-D-ribofuranoside. *J Biol Chem*275: 24279-24283, 2000.

102. **Sassoon D.** Myogenic regulatory factors: dissecting their role and regulation during vertebrate embryogenesis. *Dev Biol*156: 11-23, 1993.

103. **Schults H.** Regulation of fatty acid oxidation in heart. *J Nutr*124: 165-171, 1994.

104. **Shafi R, Iyer SP., Ellies LG., O'Donnell N., Marek KW., Chui D., Hart GW., and Marth JD.** The O-GlcNAc transferase gene resides on the X chromosome and is essential for embryonic stem cell viability and mouse ontogeny. *Proc Natl Acad Sci USA*97: 5735-5739, 2000.

105. **Shankar R, Zhu SS., and Baron AD.** Glucosamine infusion in rats mimics the beta-cell dysfunction of non-insulin-dependent diabetes mellitus. *Metabolism*47: 573-577, 1998.

106. **Shuldiner A, John C., and McLenithan JC.** Genes and pathophysiology of type 2 diabetes: more than just the Randle cycle all over again. *J Clin Invest* 116: 1414-1417, 2004.

107. **Sirito M, Walker S., Lin Q., Kozlowski MT., Klein WH., and Sawadogo M.** Members of the USF family of helix-loop-helix proteins bind DNA as homo- as well as heterodimers. *Gene Expr* 2: 231-240, 1992.

108. **Smith T, Block NE., Rhodes SJ., Konieczny SF., and Miller JB.** A unique pattern of expression of the four muscle regulatory factor proteins distinguishes somitic from embryonic, fetal and newborn mouse myogenic cells. *Development* 117: 1125 - 1133, 1993.

109. **Spector A.** Plasma lipid transport. *Clin Physiol Biochem* 2: 123-134, 1984.

110. **Stahl A.** A current review of fatty acid transport proteins (SLC27). *Pflugers Arch* 447: 722-727, 2004.

111. **Stanely W, Morgan EE., Huang H., McElfresh TA., Strek JP., Okere IC., Chandler MP., Cheng J., Dyck JRB., and Lopaschuk GD.** Malonyl-CoA decarboxylase inhibition suppresses fatty acid oxidation and reduces lactate

production during demand-induced ischemia. *Am J Physiol Heart Circ Physiol* 289: H2304-H2309, 2005.

112. **Steyn N, Bradshaw D., Norman R., Joubert J., Schneider M., and Steyn K.** Dietary changes and the health transition in South Africa: implications for health policy. *Cape Town: South African Medical Research Council*, 2006.

113. **Stryer L.** Biochemistry: Fouth Edition. *New York: Freeman and Company* 483-628, 1999.

114. **Taegtmeyer H.** Genetics of energetics: transcriptional responses in cardiac metabolism. *Ann Biomed Eng* 28: 871-876, 2000.

115. **Torres C, and Hart GW.** Topography and polypeptide distribution of terminal *N*acetylglucosamine residues on the surfaces of intact lymphocytes. Evidence for O-linked GlcNAc. *J Biol Chem* 259: 3308-3317, 1984.

116. **Trost S, Omens JH., Karlon WJ., Meyer M., Mestril R., Covell JW., and Dillmann WH.** Protection Against Myocardial Dysfunction After a Brief Ischemic Period inTransgenic Mice Expressing Inducible Heat Shock Protein 70. *J Clin Invest* 101: 855-862, 1998.

117. **Van Bilson M, Van der Vusse GJ., Gilde AJ., Lindhout M., and van der Lee KA.** Peroxisome proliferator-activated receptors: lipid binding proteins controlling gene expression. *Mol Cell Biol*239: 131-138, 2002.

118. **Van der Vusse G, van Bilsen M., and Glatz JF.** Cardiac fatty acid uptake and transport in health and disease. *Cardiovasc Res*45: 279-293, 2000.

119. **Viollet B, Lefrançois-Martinez AM., Henrion A., Kahn A., Raymondjean M., and Martinez A.** Immunochemical characterization and transacting properties of upstream stimulatory factor isoforms. *J Biol Chem*271: 1405-1415, 1996.

120. **Vosseller K, Wells L., Lane MD., and Hart GW.** Elevated nucleocytoplasmic glycosylation by O-GlcNAc results in insulin resistance associated with defects in Akt activation in 3T3-L1 adipocytes. *Proc Natl Acad Sci USA*99: 5313-5318, 2002.

121. **W.H.O.** Definition, Diagnosis and Classification of Diabetes Mellitus and its Complications. In: *World Health Organisation*, 1999.

122. **W.H.O.** World Health Report 2002. In: *World Health Organization*, 2002.

123. **Weigert C, Brodbeck K., Sawadogo M., Haring HU., and Schleicher ED.** Upstream stimulatory factor (USF) proteins induce human TGF-beta1 gene activation via the glucose-response element-1013/-1002 in mesangial cells: up-regulation of USF activity by the hexosamine biosynthetic pathway. *J Biol Chem* 279: 15908-15915, 2004.

124. **Weigert C, Brodbeck K., Sawadogo M., Haring HU.,and Schleicher ED.** Upstream Stimulatory Factor (USF) Proteins Induce Human TGF-β1 Gene Activation via the Glucose-response Element -1013/-1002 in Mesangial Cells. *J Biol Chem* 279: 15908-15915, 2004.

125. **Wells L, Voseller K., and Hart GW.** Glycosylation of nucleocytoplasmic proteins: signal transduction and O-GlcNAc. *Science* 291: 2376-2378, 2001.

126. **Wild S, Roglic G., Green A., Sicree R., and King H.** Global prevalence of diabetes estimates for the year 2000 and projections for 2030. *Diabetes Care* 27: 1047-1053, 2004.

127. **Wilson P, D'Agostino RB., Sullivan L., Parise H., and Kannel WB.** Overweight and obesity as determinants of cardiovascular risk: the Framingham experience. *Arch Intern Med* 162: 1867-1872, 2002.

128. **Winz R, Hess D., Aebersold R., and Brownsey W.** Unique structural features and differential phosphorylation of the 280-kDa component (isozyme) of rat liver acetyl-CoA carboxylase. *J Biol Chem* 269: 14438 - 14445, 1994.

129. **Yamashita H, Takenoshita M., Sakurai M., Bruick RK., Henzel WJ., Shillinglaw W., Arnot D., and Uyeda K.** A glucose-responsive transcription factor that regulates carbohydrate metabolism in the liver. *Proc Natl Acad Sci USA* 98: 9116-9121, 2001.

130. **Young M, Goodwin GW., Ying J., Guthrie P., Wilson CR., Laws FA., and Taegtmeyer H.** Regulation of cardiac and skeletal muscle malonyl-CoA decarboxylase by fatty acids. *Am J Physiol Endocrinol Metab* 280: E471-E479, 2001.

131. **Yuan H, Wong LS., Bhattacharya M., Ma C., Zarafani M., Yao M., Schneider M., Pitas RE., and Martins-Green M.** The effects of second-hand

smoke on biological processes important in atherogenesis. *BMC Cardiovasc Disord* 7: 1-16, 2007.

132. **Zachara N, and Hart GW.** Cell signaling, the essential role of O-GlcNAc! *Biochim Biophys Acta* 1761: 599-617, 2006.

133. **Zhang S, and Kim, KH.** Acetyl-CoA carboxylase is essential for nutrient-induced insulin secretion. *Biochem Biophys Res Commun* 229: 701-705, 1996.

Chapter 5

Appendix

Appendix 1: Preparation of modified RIPA buffer

Preparation notes:

Label eppendorf tubes (±98).

Be sure to keep all inhibitors on ice and to add them last as indicated in the protocol.

Many of the reagents have been made up before use.

For 100ml modified RIPA buffer:

1. Prepare 50 mM Tris-HCl (a buffering agent that prevents protein denaturation):
    - Add 790 mg Tris to 75 ml distilled H_20. Add 900 mg NaCl and stir. pH to 7.4 using HCl.

2. Add 10 ml of 10% NP-40 to the solution. (Made up previously)

3. Add 2.5 ml of 10% Na-deoxycholate (an ionic detergent to extract protein, **protect from light**) and stir. (Made up previously in H_20)

4. Add 1 ml 100 mM EDTA pH 7.4 (Acts as a calcium chelator). (Made up previously)

5. Now add the following protease inhibitors:
    - Phenylmethylsulfonyl flouoride (PMSF) – 200 mM stock made up in isopropanol and stored at room temperature (extremely short half life in aqueous solutions)
    - Leupeptin (1 mg/ml in H_20)
    - SBT1 (5 mg/ml in H_20)
    - Benzamidine (1 M)

(All of the above are stored in the freezer with the exception of PMSF which is available as a stock)

6. Add the following protease phosphatase inhibitors:
    - Activated Na_3VO_4 – 200 mM stock made up in H_2O (stored in freezer along with the protease inhibitors)
    - NaF (200 mM stock) – (Made up previously)

(Note: Do not at phosphatase inhibitors if lysates are to be used for phosphatase assays)

7. Add 1 ml of Triton X-100.

8. Make up to 100 ml with distilled H_2O using a graduated cylinder.

9. Aliquot 1 ml of RIPA buffer into each eppendorf tube before finally storing at -20℃

Final concentrations:

- Tris-HCl: 50 mM
- NP-40: 1%
- Na-deoxycholate: 0.25%
- EDTA: 1 mM
- PMSF: 1 mM
- Leupeptin: 1 µg/ml
- SBT1: 4 µg/ml
- Benzamidine: 1 mM
- Na_3VO_4: 1 mM
- NaF: 1 mM

Appendix 2: Bradford protein quantification and sample preparation

Bradford reagent (5x concentrated):

Dilute 500 mg of Coomassie Brilliant blue G in 250 ml 95% ethanol.

Add 500 ml of phosphoric acid before mixing thoroughly.

Make up to one liter with distilled H_2O (dH_2O).

Filter and store at 4℃.

Bradford working solution:

Dilute stock in a 1:5 ratio with dH_2O.

Filter using 2 filter papers (at the same time).

Solution should be a light brown color.

Bradford method:

- Thaw 1 mg/ml BSA stock solution.
- Thaw protein samples if in -80℃ freezer. Keep on ice at all times.
- Make up a working solution of 100 µl BSA:400 µl dH_2O. Vortex mixture.
- Mark 7 microfuge tubes for the standards as well as tubes for the samples to be tested.

- Now add BSA and water to marker microfuge tubes as follows:

Blank:	0 µl BSA	100 µl dH_2O	
2 µl protein:	10 µl BSA	90 µl dH_2O	
4 µl protein:	20 µl BSA	80 µl dH_2O	
8 µl protein:	40 µl BSA	60 µl dH_2O	
12 µl protein:	60 µl BSA	40 µl dH_2O	
16 µl protein:	80 µl BSA	20 µl dH_2O	
20 µl protein:	100 µl BSA	0 µl dH_2O	
Each sample:	0 µl BSA	95 µl H_20	5 µl of sample protein

- Briefly vortex all the tubes.
- Now add 900 µl of Bradford reagent to each microfuge tube. Vortex again.
- Let the solutions stand for ~5 minutes (switch on the spectrophotometer in the meantime).
- Read absorbencies, twice each, at 595 nm.
    - If sample values fall outside the range of the highest standard then dilute with RIPA buffer.
- Make use of Excel to make a linear plot of absorbencies and then calculate the amount of each sample to be added to aliquots.

Sample preparation:

- Begin by setting beaker of water to boil.
    - Remember to keep protein samples on ice at this point.
- Make up a stock solution containing 850 µl of sample buffer and 150 µl of mercaptoethanol.
- Vortex the solution.
- Calculate the number of sample sets needed, each containing one representative of each protein sample.
- Add sample buffer to each aliquot (do so under the fume hood to avoid exposure to harmful fumes).
- Add a volume of sample buffer equal to 1/3 of the final volume.
- Now add the amount of sample calculated previously to each respective microfuge tube.
- Punch small pin size holes in each tube then place in boiling water to stand for a period of 5 minutes.
- Spin tubes for a moment (~5 seconds) using the tabletop centrifuge.
- Samples can now be stored at -80℃.

Use of samples:

In the case that samples have been stored in the -80℃ freezer:

- Start by bringing a beaker of water to the boil.
- Remove samples from the freezer.
- Make sure that small pin size holes have been punched in the top of each tube.
- Place in boiling water for a period of 5 minutes.
- Spin down momentarily (20 seconds) on the tabletop centrifuge (take care not to over centrifuge, especially if samples have been obtained from tissue.
- Samples can now be used for Western blotting.

Appendix 3: Electrotransfer of proteins (Semi-dry apparatus)

Solutions for PVDF membrane

Anode buffer 1:

0.3 M Tris-base, pH 10.4

20% methanol

Anode buffer 2:

25 mM Tris-base, pH 10.4

20% Methanol

Cathode buffer:

25 mM Tris-base

40 mM ε-aminohexanoic acid

pH to 9.4

Add 20% methanol

Need 8 Whatman 3MM papers and 1 PVDF membrane per gel cut to the required size.

1. Soak PVDF membrane in methanol for 15 seconds. Put the membrane in slowly, allowing it to soak by osmosis and prevent air bubbles from being trapped.

2. Soak 3 Whatman papers in anode buffer 1.

3. Soak 1 Whatman paper in anode buffer 2.

4. Soak 4 Whatman paper in cathode buffer.

5. On the anode plate of the semi-dry apparatus put the 3 papers from step 2 (anode 1), roll with a glass tube.

6. Add 1 paper from step 3 (anode 2) and roll, making sure to remove bubbles.

7. Add the PVDF membrane and roll gently.

8. Take the gel with the proteins that have been electrophoresed and soak it in anode buffer 2. After soaking the gel, place it on top of the PVDF membrane.

9. Roll the gel with a wet tube making sure remove any bubbles.

10. Add the 4 Whatman papers from step 4 (cathode) on top of the gel and roll it with the glass tube.

11. Close the apparatus with the lid and set it to transfer for 1 hour at 15 volts and a current of 0.5 A.

12. After the electrotransfer is complete fix the protein to the PVDF membrane by placing it in methanol for a few seconds

Appendix 4: O-GlcNAc Western blotting and detection

Note: The following description is reproduced as supplied by the O-GlcNAc Western blot detection kit (Pierce, catalogue number 24565, Rockford, Illinois).

Material Preparation:

(All reagents are supplied in the O-GlcNAc Western blot Detection Kit)

Wash Buffer	Reconstitute one BupH™ Phosphate Buffer Saline (PBS) pack with 500 ml of ultrapure water and add 2.5 ml of 10% Tween®-20 for a final concentration of ~0.05%.
Blocking Buffer	Dilute the 10x “Dilution buffer” (also functions as blocking buffer) to 1x in Wash buffer (e.g. 1 ml of 10x Dilution Buffer to 9 ml of Wash buffer).
Goat Anti-Mouse IgM -HRP Conjugate	Prepare a 1 mg/ml stock solution by reconstituting the antibody in 75 µl of ultrapure water. Aliquot 6 µl the secondary antibody into separate micofuge tubes and add an equal volume of glycerol per aliquot. Store the aliquots at -20°C. By adding glycerol the final concentration of each aliquot changes to 0.5 mg/ml.

Procedure:

1. Remove PVDF membrane from the transfer apparatus and block nonspecific sites on the membrane by completely immersing the membrane with the blocking membrane (approximately 50 ml) at room temperature (RT) overnight at 4°C.

2. Prepare a 1:5,000 dilution of the anti-*O*-GlcNAc monoclonal antibody in blocking buffer.

3. Remove blocking buffer and add ~ 30 ml of the diluted antibody to the membrane. Incubate the blot overnight at 4°C. Alternatively, we used 2 µl of primary antibody in 10 ml of blocking buffer in a 50 ml Falcon tube and left the membrane to incubate overnight at 4°C.

4. Wash the membrane six times by completely immersing in wash buffer (approximately 50 ml) and shaking for 5 minutes.

5. Prepare a 10 µg/ml secondary antibody solution by diluting the 0.5 mg/ml stock solution 1:100 in blocking buffer. Prepare approximately 30 ml of a 1:5,000 dilution of the 10 µg/ml goat anti-mouse IgM-HRP in blocking buffer. For 30 ml of blocking buffer we added 12 µl of secondary antibody.

6. Remove wash buffer, add the diluted secondary antibody and incubate for 1 hour at room temperature with gentle shaking.

7. Wash the membrane 6 times by completely immersing the membrane in wash buffer (approximately 50 ml) and shaking for 5 minutes.

8. Prepare SuperSignal® West Dura Working Solution by mixing 5 ml of the Stable Peroxide Solution and 5 ml of the Luminol/Enhancer solution. Apply working solution to the membrane and incubate for 5 minutes at room temperature. Use 0.125 ml substrate solution per cm^2 of membrane.

9. Remove membrane from working solution and place in a plastic membrane protector. (We used two pieces of acetate).

10. Place the protected membrane in a film cassette with the protein side facing up.

11. The membrane was exposed to Hyperfilm (Amersham, Buckinghamshire, UK) in a dark room for up to 7 seconds and then placed in developer for ± 30 seconds. The film was washed and fixed.

Appendix 5: GFAT Western blotting and detection

Buffers used:

10x Tris Buffer Saline (TBS): (5 litres)

121 g Tris

40 g NaCl

pH solution to 7.6

TBS-T Wash Buffer — Add 10 ml of 10x TBS to 90 ml of ultrapure or distilled water and then add 1 ml of Tween-20.

Blocking Buffer — Add 5 mg of milk powder (Elite skim milk powder) to 100 ml of TBS-T.

Procedure:

1. Remove PVDF (Millipore, Billerica, USA) membrane from the transfer apparatus and wash the membrane 3 times with TBS-T for 5 minutes.

2. Block nonspecific sites on the membrane by completely immersing the membrane with the blocking membrane (approximately 50 ml) at room temperature (RT) overnight at 4°C.

3. Prepare a 1:3,000 dilution of the GFAT antibody in blocking buffer.

4. Incubate the blot overnight at 4°C. We used 17 ul of primary antibody in 5 ml of blocking buffer in a 50 ml Falcon tube and left the membrane to incubate overnight at 4°C.

5. Wash the membrane six times by completely immersing in TBS-T wash buffer (approximately 50 ml) and agitating for 5 minutes.

6. Prepare approximately 1:2,000 dilution of goat anti-rabbit-horse radish peroxidase in blocking buffer. For 5 ml of blocking buffer we added 5 µl of secondary antibody.

7. Remove wash buffer, add the diluted secondary antibody and incubate for 1 hour at room temperature with gentle shaking.

8. Wash the membrane six times by completely immersing the membrane in TBS-T wash buffer (approximately 50 ml) and shaking for 5 minutes.

9. Wash the membrane for 15 minutes with TBS.

10. Add 0.5 ml of ECL Reagent 1 to the membrane and then add ECL reagent 2 to the membrane. Make sure to spread the ECL reagents over the whole membrane. Incubate for 1 minute at room temperature while continuously washing the ECL reagent mixture over the membrane.

11. Remove membrane from ECL reagent and place in a plastic membrane protector (we used two pieces of acetate).

12. Place the protected membrane in a film cassette with the protein side facing up.

13. The membrane was exposed to Hyperfilm (Amersham, Buckinghamshire, UK) in a dark room for up to ± 7 minutes and then placed in developer for ± 30 seconds. The film was washed and fixed.

Appendix 6: β-Actin Western blotting and detection

Buffers used:

TBS-T Wash Buffer	Add 10 ml of 10x TBS to 90 ml of ultrapure or distilled water and then add 1 ml of Tween-20.
Blocking Buffer	Add 5 mg of milk powder (Elite skim milk powder) to 100 ml of TBS-T.

Procedure:

1. Remove PVDF (Millipore, Billerica, USA) membrane from the transfer apparatus and wash the membrane 3 times with TBS-T for 5 minutes.

2. Block nonspecific sites on the membrane by completely immersing the membrane with the blocking membrane (approximately 50 ml) at room temperature (RT) overnight at 4°C.

3. Prepare a 1:1,000 dilution of the anti-β-Actin monoclonal antibody (Cell Signaling, Danvers, MA, USA) in blocking buffer.

4. Incubate the blot overnight at 4°C. We used 5 µl of primary antibody in 5 ml of blocking buffer in a 50 ml Falcon tube and left the membrane to incubate overnight at 4°C.

5. Wash the membrane five times by completely immersing in TBS-T wash buffer (approximately 50 ml) and agitating for 5 minutes.

6. Prepare approximately 1:2,000 dilution of goat anti-rabbit-horse radish peroxidase in blocking buffer. For 5 ml of blocking buffer we added 5 µl of secondary antibody.

7. Remove wash buffer, add the diluted secondary antibody and incubate for 1 hour at room temperature with gentle shaking.

8. Wash the membrane 3 times by completely immersing the membrane in TBS-T wash buffer (approximately 50 ml) and agitating for 5 minutes.

9. Wash the membrane for 15 minutes with TBS.

10. Add 0.5 ml of ECL reagent 1 to the membrane and then add ECL reagent 2 to the membrane. Make sure to spread the ECL reagents over the whole membrane. Incubate for 1 minute at room temperature while continuously washing the ECL reagent mixture over the membrane.

11. Remove membrane from ECL reagent and place in a plastic membrane protector (we used two pieces of acetate).

12. Place the protected membrane in a film cassette with the protein side facing up.

13. The membrane was exposed to Hyperfilm (Amersham, Buckinghamshire, UK) in a dark room for up to ± 7 minutes and then placed in developer for ± 30 seconds. The film was washed and fixed.

Appendix 7: Stripping protocol

1. Make up the following solution:

    100 mM β-Mercaptoethanol: 700 ml/100 ml

    2% SDS: 20 ml/100 ml (from 10% stock)

    62.5 mM Tris-HCl pH 6.7: 0.757 g/100 ml

    Make up to 100 ml with H_20

2. Incubate membrane in solution at 60°C for 30-60 min with occasional agitation.

3. Wash the membrane in TBS-Tween before blocking in 5% milk.